



# **UNIVERSITY OF NAIROBI**

**FACULTY OF ENGINEERING**

**DEPARTMENT OF ELECTRICAL AND INFORMATION ENGINEERING**

## **BER CHARACTERIZATION OF FREQUENCY-CODED MULTIPLE RANK MODULATION**

**BY**

**NYANJOM JACK ONYANGO**

**F56/7211/2017**

A Thesis submitted in partial fulfilment for the Degree of Master of Science in Electrical and Electronic Engineering in the Department of Electrical and Information Engineering of the University of Nairobi

**June 2022**

### Declaration of Originality

Name of student: NYANJOM JACK ONYANGO

Registration: F56/7211/2017

Faculty: ENGINEERING

Department: ELECTRICAL AND INFORMATION ENGINEERING

Course Name: MSc. ELECTRICAL AND ELECTRONIC ENGINEERING

Title of work: BER CHARACTERIZATION OF FREQUENCY-CODED MULTIPLE RANK MODULATION

I declare that this thesis is my original work and has not been submitted elsewhere for examination, the award of a degree or publication. Where other works or my work has been used, this has properly been acknowledged and referenced per the University of Nairobi's requirements.

Signature:  .....

Date: 23<sup>rd</sup> June 2022 .....

This thesis has been submitted for examination with our approval as university supervisors.

Dr. Peter O. Akuon

University of Nairobi

Signature:  .....

Date: 5-7-2022 .....

Prof. Vitalis K. Oduol

University of Nairobi

Signature:  .....

Date: 6 / 7 / 2022 .....

## **DEDICATION**

My family, fellow researchers, and friends, I dedicate this work to you.

## **ACKNOWLEDGEMENT**

Firstly, my deepest gratitude goes to the Almighty God who has made all this possible.

My family, who have been a constant source of motivation and encouragement during the master's degree, I sincerely thank you. I am extremely grateful to my parents, Gordon Nyanjom and Joyce Nyanjom, who instilled in me the vital characteristics of fortitude and diligence, among others. My siblings Rael, Jane, and Eric, as well as my wife Stacey, I appreciate your important support and encouragement throughout the road.

I'd like to extend my appreciation to Kenya Education Network (KENET) for the support accorded during the research period by providing infrastructure support as well as financial support to facilitate carrying out the research work.

Above all, I am thankful to my supervisor, Dr. Peter O. Akuon, who has been exceedingly accessible and hospitable throughout the master's program. He has provided several ideas and has been a consistent source of encouragement, typically providing good comments in a timely manner.

Lastly, I'd also like to appreciate the professional guidance received from Prof. Vitalis K. Oduol whose guidance and checks ought to be mentioned and appreciated as well.

## TABLE OF CONTENTS

DEDICATION .....	ii
ACKNOWLEDGEMENT .....	iii
LIST OF TABLES .....	vi
LIST OF FIGURES .....	vii
LIST OF APPENDICES.....	viii
LIST OF ABBREVIATIONS.....	ix
ABSTRACT.....	xi
CHAPTER 1: INTRODUCTION .....	1
1.1 Background .....	1
1.2 Problem Statement .....	2
1.3 Research Objectives .....	3
1.3.1 Main Research Objective.....	3
1.3.2 Specific Research Objectives.....	3
1.4 Justification for the Study .....	4
1.5 Scope of work.....	4
1.6 Thesis Organization.....	5
CHAPTER 2: LITERATURE REVIEW .....	6
2.1 Orthogonal Frequency Division Multiplexing.....	6
2.1.1 OFDM Transceiver .....	10
2.2 Spatial Modulation .....	12
2.2.1 SM Transmitter .....	14
2.2.2 SM Channel .....	16
2.2.3 SM Receiver.....	17
2.3 Generalized Spatial Modulation.....	19
2.4 Space Shift Keying.....	19
2.5 Generalized Space Shift Keying .....	19
2.6 Multiple Active Spatial Modulation.....	20
2.7 Extended Spatial Modulation.....	20
2.8 Layered Spatial Modulation .....	21
2.9 Subcarrier-Index Modulation.....	21

2.10	Multiple Rank Modulation .....	22
2.11	Motivation .....	24
CHAPTER 3: METHODOLOGY .....		26
3.1	FMRM System Model.....	26
3.2	Signal Transmission.....	27
3.2.1	Rician Channel Transmission .....	29
3.3	FMRM Sample Mapper .....	30
3.4	Signal Detection .....	30
3.4.1	Maximum Likelihood (ML).....	30
3.4.2	Selection Combining (SC) .....	32
3.5	System Performance Analysis.....	33
3.5.1	Bit Error Probability .....	34
3.5.2	Validation Framework .....	35
CHAPTER 4: RESULTS AND DISCUSSIONS .....		39
4.1	FMRM at Varying Data Rates .....	39
4.2	FMRM Comparison with M-QAM.....	40
4.3	FMRM Comparison with SIM.....	41
4.4	FMRM Threshold Detector.....	42
4.5	FMRM with SC Diversity .....	43
4.6	FMRM with SC Diversity and Antenna Correlation .....	45
4.7	FMRM at Varying Data Rates - Rician Channel .....	47
4.8	FMRM Threshold Detector - Rician Channel.....	48
CHAPTER 5: CONCLUSION AND RECOMMENDATIONS .....		50
5.1	Conclusion.....	50
5.2	Recommendations .....	53
REFERENCES .....		54
APPENDICES .....		59
Appendix A – Author’s Publications.....		59
A1.	IEEE AFRICON 2021 (Arusha, Tanzania).....	59
A2.	UoN Architecture & Engineering Conference 2020 (Nairobi, Kenya) .....	64
A3.	UoN Architecture & Engineering Conference 2019 (Nairobi, Kenya) .....	67

## LIST OF TABLES

Table 2.1 – Merits and Demerits of OFDM.....	9
Table 2.2 – S.M Mapping Table .....	16
Table 2.3 – Merits and Demerits of SM .....	18
Table 2.4 – Merits and Demerits of SIM .....	22
Table 2.5 – Merits and Demerits of MRM .....	24
Table 3.1 – Mapping Table for FMRM .....	30
Table 5.1 – Merits and Demerits of FMRM .....	50

## LIST OF FIGURES

Figure 2.1 - Block illustration of an OFDM Transceiver .....	10
Figure 2.2 - SM Transmission Techniques based on ON/OFF Principle .....	13
Figure 2.3 – Spatial Modulation constellation diagram in three-dimension.....	13
Figure 2.4 - How Spatial Modulation Works.....	15
Figure 2.5 - MRM System Model [2] .....	23
Figure 3.1 – FMRM System Model.....	26
Figure 3.2 – 3Bits BPSK Transmission .....	34
Figure 4.1 – Comparison of FMRM at different data rates .....	39
Figure 4.2 – Comparison of FMRM with MQAM .....	40
Figure 4.3 – Comparison of FMRM with SIM.....	41
Figure 4.4(a) – Varying FMRM Threshold Detection: 2Bits Tx.....	42
Figure 4.4(b) – Varying FMRM Threshold Detection: 3Bits Tx.....	43
Figure 4.5(a) – FMRM with SC Diversity: 2Bits Tx.....	44
Figure 4.5(b) – FMRM with SC Diversity: 3Bits Tx.....	44
Figure 4.6(a) – FMRM with SC Diversity and Antenna Correlation: 2Bits Tx .....	46
Figure 4.6(b) – FMRM with SC Diversity and Antenna Correlation: 3Bitx Tx.....	46
Figure 4.7 – Comparison of FMRM at different data rates: Rician Channel .....	47
Figure 4.8 – Varying FMRM Threshold Detection: Rician Channel .....	48



## LIST OF APPENDICES

Appendix A: Author's Publications .....	59
A1. IEEE AFRICON 2021 (Arusha, Tanzania) .....	59
A2. UoN Architecture & Engineering Conference 2020 (Nairobi, Kenya) .....	64
A3. UoN Architecture & Engineering Conference 2019 (Nairobi, Kenya) .....	67

## LIST OF ABBREVIATIONS

AFC	Automatic Frequency Control
AM	Amplitude Modulation
BEP	Bit Error Probability
BER	Bit Error Rate
BERP	Bit Error Rate Probability
BPS/bps	Bits Per Second
BPSK	Binary Phase Shift Keying
CP	Coded Orthogonal Frequency Division Multiplexing
CSI	Cyclic Prefix
CSI	Channel State Information
DFT	Discrete Fourier Transform
DSM	Double Spatial Modulation
ESM	Enhanced/Extended Spatial Modulation
FDM	Frequency Division Multiplexing
FDMA	Frequency Division Multiple Access
FEC	Forward Error Correction
FFT	Fast Fourier Transform
FM	Frequency Modulation
FMRM	Frequency-Coded Multiple Rank Modulation
GSM	Generalized Spatial Modulation
GSSK	Generalized Space Shift Keying
IAS	Inter Antenna Synchronization
ICI	Inter-channel Interference
IFFT	Inverse Fast Fourier Transform
IoT	Internet of Things
ISI	Inter-Symbol Interference
LAN	Local Area Network
LSM	Layered Spatial Modulation
MASM	Multiple Active Spatial Modulation

MIMO	Multiple Input Multiple Output
MISO	Multiple Input Single Output
ML	Maximum Likelihood
MRM	Multiple Rank Modulation
MRRC	Maximum Receive Ratio Combining
OFDM	Orthogonal Frequency Division Multiplexing
PABX	Private Automation Branch Exchange
PCM	Pulse-Coded Modulation
PCSM	Polar Coded Spatial Modulation
PRP	Power Reallocation Policy
PSK	Phase Shift Keying
PSP	Power Saving Policy
QAM	Quadrature Amplitude Modulation
QPSK	Quadrature Phase Shift Keying
RF	Radio Frequency
SDMA	Space Division Multiple Access
SE	Spectral Efficiency
SIM	Subcarrier Index Modulation
SISO	Single Input Single Output
SM	Spatial Modulation
SSK	Spatial Shift Keying
UEP	Unequal Error Protection

## ABSTRACT

The growing need for higher rates of data transmission has made Multiple-Output Multiple-Input (MIMO) systems become the main focus for communication systems. In this work, a signal transmission technique is proposed where information to the receiver is transmitted via different ranks of frequency subcarriers i.e., Frequency-Coded Multiple Rank Modulation (FMRM). In FMRM, the input information bits stream determines the number of subcarriers required. The ranking modulator receives a random bitstream of information as input. Instead of the channel index, the receiver detects the number of frequency subcarriers in an OFDM scheme. A system mapper is used to pre-set and know the pattern of frequency subcarriers at the receiver. The bits in the frequency domain can only be decoded using the rank information.

A threshold detector that utilizes the optimal power required for detection, employed at the receiver, is used to accurately identify the transmitted signals. A desirable value for the threshold detector is obtained for both cases of Gaussian and Fading channels i.e., 0.6 and 0.3 respectively. Analytical upper constraints on the FMRM system's information-theoretic approach are derived for validation and then compared to simulation findings for related systems like Subcarrier Index Modulation (SIM) and alternative transmission techniques at similar data rates e.g., BPSK and M-QAM which show tractable performance (FMRM has a 9 dB gain when compared with BPSK, a 6 dB gain when compared with 4-QAM and a 1 dB gain when compared with 8-QAM).

When comparing different transmission data rates (1bit per second (bps), 2 bps and 3 bps), a signal to noise ratio deviation of approximately 6 dB is observed between a 1 bps and 2 bps transmission and similarly a deviation of approximately 9 dB is observed between 2 bps and 3 bps transmission. Further, the antenna correlation effect on the receive antennas is investigated and system performance is shown for the same vis a vis non-antenna correlation with a deviation of the two scenarios being approximately 4dB. In addition to the wireless channel, the frequency chains also modulate the information sent which improves transmission speeds, which not only makes the FMRM system better as a very reliable system for next generation wireless networks that are built on faster transmission speeds with very low latency but also makes FMRM a better system for use in information security operations.

## CHAPTER 1: INTRODUCTION

### 1.1 Background

High data rates, being a desideratum, in systems of wireless communication is on the rise and requires transmission methods that attain high spectral effectiveness. In the recent past, it was noted that the MIMO wireless communication systems, which utilizes several antennas at the reception and transmission points to realize antenna gain and diversity gain, seem to be certain in the accelerated development of applications with high data rates. MIMO systems of communication have received substantial attention from commercial firms and researchers because of their potential to substantially increase spectral efficiency and concurrently send specific information to the various users in the wireless communication system [1]. MIMO systems take advantage of a phenomenon of radio-wave propagation known as multipath where communicated signals rebounds off the ceilings, walls, and various objects, reaching the recipient antenna numerous times through different dimensions and at slightly dissimilar times.

MIMO technology assumes multipath behavior by utilizing multiple “smart” receivers and transmitters with an additional spatial dimension to substantially increase range and performance. MIMO ensures antennas work more efficient by enabling them to bring together data streams coming from various paths and at varied times to effectively enhance receiver signal-capturing potential. Smart antennas make use of spatial diversity technology, which makes surplus antennas work better. If there exist more antennas than spatial streams, the supplementary antennas could increase range and add receiver diversity [1]. As an outcome of the utilization of multiple antennas, the MIMO communication system is able to considerably enhance the capacity of a specific channel. By amplifying the number of transmission and reception antennas it is likely to linearly raise the output of the channel with each pair of antennas supplemented to the system.

Conventional MIMO systems utilize a maximum of eight antennas at both the transmitter and receiver side [2]. With massive MIMO and the selection of prototype implemented, a maximum of 256 base stations and 32 user equipment antennas for 5G new radio can be implemented [3]. As the bandwidth of the spectrum becomes a more valuable product for radio systems, methods

are required to use the available bandwidth more efficiently. One of these methods is MIMO wireless technology. Satellite technology advancement has necessitated a rise in data rate transmissions. To meet communication requirements, satellites are forced to operate in high-frequency bands such as Ka-band [4]. Several factors impact data transmission speeds, ranging from technical factors such as frequency range and modulation technology to implementation elements like transceiver complexity or scalability [5].

A key technology that will help achieve the desired high data rates is Multiple Rank Modulation (MRM). A transmission method and system of multiple rank modulation in a MISO or a MIMO system is given which entails reception at a transmitter, a plurality of bits signal and categorizing the signal received into a signal modulation and a rank index bit block. The bit block modulation signal is programmed in a system for further transmission. The rank index bit block helps in selecting a rank to be initiated, in which the activated rank has no less than one activated transmitter projection and the programmed bit block signal modulation is conveyed via the stimulated rank being not less than one initiated antenna for transmission. The conveyed encoded bit block for signal modulation is acknowledged via the receiving antenna and a rank index, as well as a symbol of transmission projected from the received signal. The bit block signal variation is decoded finally.

## **1.2 Problem Statement**

With the growing demand for higher data rates, MIMO systems have become the main focus for communication systems. Spatial modulation (SM) being a recent technology has several advantages over other MIMO schemes. In addition to the modulation signal, SM utilizes antenna index as a source of information to increase transmission capacity, avoid some level of synchronization and Inter-Channel Interference (ICI). However, the utilization of an index for the transmission antenna as a source of data has the implication that if the channels look alike, then spatial information may be lost completely. This is because just like all the variants of SM technology for instance Space Shift Keying (SSK), Double Spatial Modulation (DSM), and Generalized Space Shift Keying (GSSK), the SM detector uses the shape of each channel to

detect spatial information. In fact, there may be cases in the user market that may lead to the reception of signals that look alike due to the similarity of channels e.g., in signal correlation [6].

In Enhanced Spatial Modulation (ESM), the received signal power can be used to detect the spatial information where each activated transmit antenna transmits at a known power level. However, this leads to other implementation implications at the transmission system and feedback may be required from the recipient system. Also, in Polar Coded Spatial Modulation (PCSM), different rates can be used to transmit known frozen bits and then use the rate or capacity information to decode the spatial bits with minimal error or in the control channel. However, coset-coding is required to achieve this technique [6]. Due to this, an enhanced Spatial Modulation technique as well as transmitting and receiving devices through the use of MRM for decreasing the high demodulation complexity and errors in the spatial domain, while providing additional capacity and data rates was introduced [6]. This was able to achieve multiple gains over the conventional SM schemes.

To further improve on the gains made by MRM, there is a need to refine it further by employing the use of frequency as a fabric in the transmission of information signals by introducing FMRM. This will have the major advantage of enhancing information security of the conveyed information while at the same time helping to achieve a reduction in the high demodulation complexity and errors encountered in the spatial domain as utilized by other SM schemes.

### **1.3 Research Objectives**

#### **1.3.1 Main Research Objective**

Characterization of the performance of a Frequency-coded Multiple Rank Modulation system.

#### **1.3.2 Specific Research Objectives**

- i. Development of a mapping strategy for FMRM.
- ii. Development of a detection mechanism for an FMRM system.
- iii. Application of Selection Combining Diversity and Correlation tests using multiple receive antennas for the FMRM system.
- iv. Performance analysis of the FMRM system in a flat-fading channel.

#### **1.4 Justification for the Study**

The next-generation wireless communication delivers much more than faster speeds, providing a range of new technical capabilities. They're critical in delivering new solutions to enhance economic development, healthcare, manufacturing, infrastructure and even delivery of government services. With the capacity to support over one million devices per square kilometer, the next-generation wireless communication enable numerous device connectivity in any given area. This means massive Internet of Things (IoT), support for mission-critical communications, more video streaming, voiced calls and quicker access to documents, photos, gaming and files in the cloud. To aid in this, the proposed FMRM system offers improved data rates as necessitated by the next generation communication systems while providing better information security operations.

Practical market application areas that can exploit FMRM include, but are not limited to, Digital Video Broadcasting (DVB); Ultra-Low Latency Communication e.g., 5G; Vehicle-to-Vehicle Communications e.g., Autonomous Vehicle Control Systems (AVCS); Indoor Propagation e.g., Indoor wireless RF channels (cordless phones, Wireless LANs & PABX-es); and Microcellular channels to enhance user capacity (low transmit powers possible allowing miniaturization of handheld terminal).

#### **1.5 Scope of work**

This work concentrates on the utilization of frequency as a fabric to study multiple rank modulation by using frequency to select an antenna rank before signal transmission is done. A threshold detector is introduced which is used to determine from which antenna the signal is coming from. An analytical framework is developed that changes the carrier frequency of the antennas after a random number of transmissions thus making it difficult for one to study the transmit patterns and gain access to information. Simulations of the whole system are then carried out using OCTAVE which is an open-source software.



## **1.6 Thesis Organization**

In the remainder of this thesis, the following sections are included; Chapter 2 looks at the literature review and the research gap identification, Chapter 3 talks about the research methodology employed to obtain results. Chapter 4 covers the results obtained from the proposed system and these are discussed in Chapter 5. Chapter 6 finalizes the FMRM discussion and offers recommendations for further work. To conclude, the references used are listed, Author's publications highlighted, and Plagiarism Checker (Turnitin) report appended.

## CHAPTER 2: LITERATURE REVIEW

Index modulation (IM) is a novel digital modulation system that communicates information by using the on-off state of transmission entities such as antennas, subcarriers, spreading codes, and signal constellations [7]. The fact that extra information is implicitly conveyed over the produced signal at little or no power cost is a distinctive feature of IM, allowing for significant advances in spectral efficiency (SE) and energy efficiency (EE). Because of these benefits, IM looks to be a viable choice with the ability to interact with cognitive radio, relay networks, and physical layer security (PLS) with high SE/EE to design future wireless networks. Long Term Evolution has employed the IM concept for hybrid automated repeat request-acknowledgement (HARQ-ACK) and scheduling request (SR) reporting through physical uplink control channel (PUCCH) format 1a/1b. The HARQ-ACK is broadcast especially on the SR PUCCH channel, the status of which transmits the SR implicitly [8].

### 2.1 Orthogonal Frequency Division Multiplexing

OFDM is defined as a technique for transmission in a multicarrier platform, that separates the existing range of carrier frequency into various carriers, where every carrier is being controlled by a data stream of low rate [9]. Accordingly, as a wideband communication system, OFDM has become well-known due to its capacity to endure the channel settings with high severity with no multifaceted filters for equalization; for example, narrowband interference, diminution of high-frequency rates in an extensive copper wire and fading that is selective on frequency because of the multipath nature. The equality of channel is made simple since OFDM might be perceived as utilizing many gradually moderated signals that are narrowband other than a faster-controlled broadband signal. A rate of symbol that is low allows the utilization of an interval of the guard between various symbols to be affordable, allowing it to deal with time-variation as well as remove any Inter-Channel Interference (ICI) and Inter-Symbol Interference (ISI) [10-19].

A major purpose for utilizing OFDM would be to amplify the strength of the signal in the context of narrowband interference or fading that is frequency selective. Within a unit system of a carrier, an interferer or a unit fade could lead to failure of the whole link. However, in a system of multicarrier design, just a minimal portion of the sub-carriers would be impacted. Coding of rectification of error is used to rectify subcarriers with small errors. Orthogonality specifies that a

detailed mathematical association exist between the carriers' regularities within the communication system. Accordingly, in an ordinary FDM communication system, most carriers are disintegrated such that the signals could be got through the use of conventional demodulators and filters. The guard bands in such reception points are instituted among the various carriers within the domain frequency, which consequently lowers the spectrum efficiency. In the context of an OFDM communication signal, arranging the carriers is possible after which the peripheral bands of the specific carriers would overlay, and the signals would still be captured without the interference of the next carrier thus the requirement that the carriers need to be orthogonal.

P.M. Ebert and S. B. Weinstein proposed a Discrete Fourier Transform (DFT) technique in carrying out the basic band demodulation as well as modulation [20]. Accordingly, DFT is deemed as an effective algorithm for the dispensation of signals that helps in the elimination of the sub-carrier oscillators' banks. The authors' utilized space guard instituted among symbols to deal with the ISI and ICI issues. The arrangement could not arrive at the best orthogonality among sub-carriers through a diverse channel. A computationally efficient DFT implementation, the Fast Fourier Transform (FFT), is based on DFT. Demodulation and modulation methods used in OFDM include Inverse FFT (IFFT) and FFT [21]. Ruiz and Peled instituted Cyclical Prefix (CP) that resolves the problem of orthogonality [22]. They occupied the space guard using a cyclical elongation of the symbol of OFDM which presumed the CP is much longer than the channel response to the impulse.

Expression of the DFT that is also the low-pass equivalence of OFDM signal is as shown below.

$$X(t) = \sum_{k=0}^{N-1} X_k e^{j\frac{2\pi kt}{T}} \quad , 0 \leq t < T \quad (2.1)$$

where  $X_k$  are symbols of data which is a classification of complex numbers that represent QAM, QPSK or BPSK symbol of the baseband,  $N$  represents the subcarriers numbers while the  $T$  represents the line of the symbol of OFDM. The spacing of the subcarrier  $\frac{1}{T}$  allows them to be orthogonal throughout each period of the symbol. The order of symbols in an OFDM transmission is given by the equation below:

$$S(t) = \sum_{k=-\infty}^{+\infty} X(t - kT) \quad (2.2)$$

To evade ISI, a guard length interval  $T_g$  is introduced prior to the block of OFDM. At this intermission, a CP is communicated. The signal having the CP is therefore illustrated below

$$X(t) = \sum_{k=0}^{N-1} X_k e^{j\frac{2\pi kt}{T}} \quad , T_g \leq t < T \quad (2.3)$$

The merits and demerits of the OFDM scheme are captured in Table 2.1.

Table 2.1 - Merits and Demerits of OFDM

Merits	Demerits
<ul style="list-style-type: none"> <li>i. OFDM allows essential utilization of spectrum by creating an intersection. By separating the frequency into sub-channels that are flat fading narrowband, OFDM is more resilient to regularity fading that is selective than a unit carrier communication system.</li> <li>ii. It is capable of enduring the conditions of channels that are severe with no stratified time-domain equalization.</li> <li>iii. It can tone down the IFI and ISI through the utilization of the CP and a fading that is stimulated by the spread across multipaths.</li> <li>iv. The utilization of the right channel interleaving and coding of the symbols lost could be recovered.</li> <li>v. The equalization of the channel is usually made simple through the utilization of the equalization methods that are adaptive within a unit system of the carrier.</li> <li>vi. The system of OFDM is deemed to be quite proficient in the use of FFT methods in carrying out the functions of demodulation and modulation.</li> <li>vii. Its sensitivity is low with regards to offsetting timing of the sample than the systems of a single carrier.</li> <li>viii. Its strength against the narrowband interference of the co-channel is quite high.</li> <li>ix. The requirement of the filters on account of the subchannel receivers is not necessary unlike the traditional FDM</li> </ul>	<ul style="list-style-type: none"> <li>i. A vast dynamic range and a noisy amplitude of the OFDM amplitude makes it require amplifiers that are RF powered containing a high range of power.</li> <li>ii. It is essentially susceptible to the offset of the frequency of the carrier and drift than unit systems of the carrier are because of the DFT leakage.</li> <li>iii. It is susceptible to the shift of the Doppler.</li> <li>iv. It needs linear transmission circuitry, which has a problem of poor power competence.</li> <li>v. It has a problem of efficiency loss brought about by the cyclic prefix.</li> </ul>

## 2.1.1 OFDM Transceiver

An OFDM transceiver in block form is illustrated in Process Map 2.1 below [21].

### 2.1.1.1 OFDM Transmitter

A randomizer is utilized as a generator of a randomized bit. The FEC Encoder performs the linear encoding of the input signal using a generator matrix. Using the interleaver, existing error-correcting codes are enhanced and can now be used for burst error correction. Efficient digital information transmission of the generated analogue signal is enabled by the QAM mapper, and this amplifies the useable bandwidth by either adjusting the power level or amplitude of two signals. A converter of serial-parallel nature is used to parallelize the serial bits of data. The IFFT converts the signals contextually from of field of frequency to the context of the field of time; an IFFT transforms various multifaceted points of data, of measurement that is squared, into the equivalent points but only in the domain of time. The prearranged subcarriers numbers determine the number of sub-bands the existing spectrum is categorized [23, 24]. To alleviate the ISI problem, the CP is a copy of the IFFT's later samples number, which is inserted at the start of the frame OFDM. To improve the overall system's efficacy, it's critical to choose the least important CP [25].

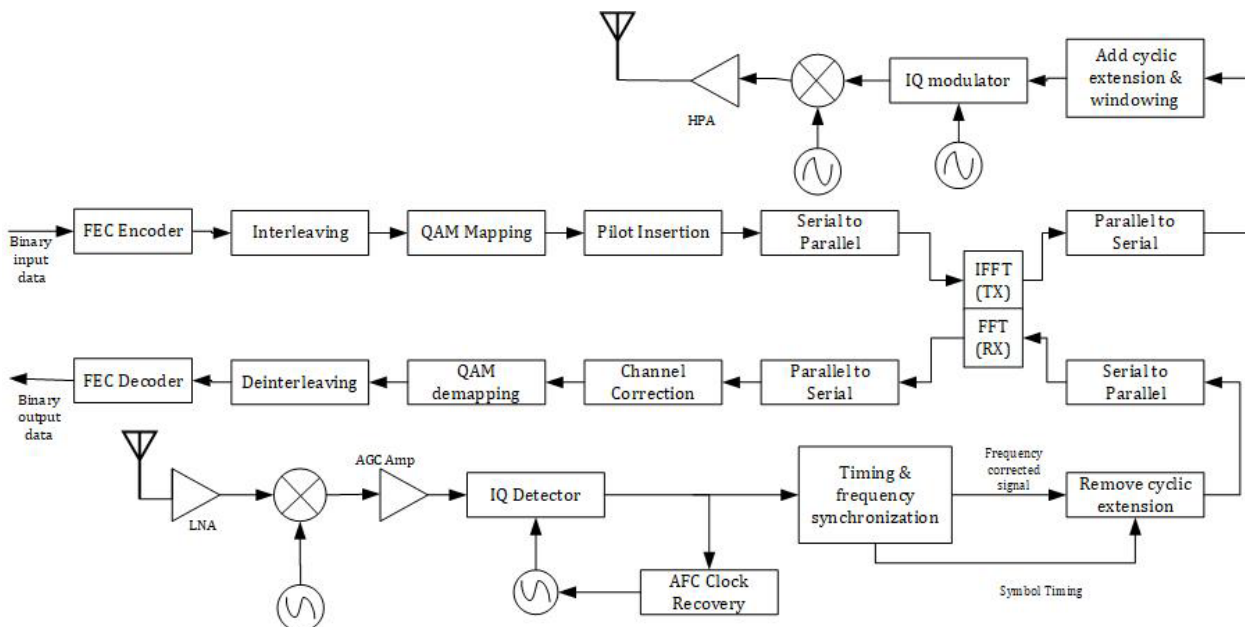


Figure 2.1 - Block illustration of an OFDM Transceiver

### 2.1.1.2 OFDM Receiver

The received signal passes through the IQ detector which converts the received baseband information into RF signals. Following that, the received signal goes via AFC clock recovery, which estimates and adjusts for frequency and phase discrepancies between the amplitude carrier wave of the received signal and the receiver's local oscillator for coherent demodulation. The receiver uses timing synchronization to determine the correct sample intervals for an inbound signal, whereas the receiver uses frequency synchronization to modify the frequency and phase of its local carrier oscillator to match the received signal. The signal received then goes through the removal of the CP and a serial form-to-parallel form system of conversion [23]. The signals are then taken via an  $N$ -point FFT to change the signal to a regularity field. Thus, the throughput of the FFT is instituted on the context of the initial output samples of the modulated signal  $M$ . Demodulation is then possible by the use of DFT, or made efficient, by FFT, which is the effectual execution that could be utilized hence, plummeting the processing period, as well as the hardware, used [26]. The FFT computes DFT with a substantial decrease in the operations levels, leaving numerous existing obsolescence in the computation of DFT [26-28].

The system of OFDM has similarity with FDMA since the multiple access by the user is realized through sectioning the existing bands into manifold frequencies, which are then assigned to various end-users. In FDMA, every end-user is naturally allocated a unit channel between 10kHz-30kHz while the minimum needed bandwidth for speech only stands at 3kHz. This additional band is to permit signals from adjacent networks to be sifted out, in order to permit any deviation in the core regularity of the receiver or transmitter. In the context of a characteristic arrangement, up to around 50 percent of the whole range is put to waste because of the additional space among networks and deteriorates as the network bandwidth narrows, and the regularity band rises. But the OFDM utilizes the spectrum more proficiently by separating the networks and ensuring that all the systems' carriers are orthogonal to each other, reducing the propensity of disturbance among the separated carriers. Coded OFDM (COFDM) is similar to OFDM save for the fact that forward error rectification is instituted to the signal prior to the intended transmission. This correction is to resolve errors in the communication emanating from the carriers that are lost from selective regularity fading, channel interference (noise) and other dissemination disturbances.

## 2.2 Spatial Modulation

SM is a multi-antenna transmission technology that assures faster data speeds (than systems of SISO) and strong performance of error even in interrelated channel settings with minimally low system complexity. SM exploits the exceptional and random features of the wireless transmission channel. This could be realized by implementing a modest and operative coding method that creates a mapping of one-to-one amongst block-data bits to be conveyed and the spatial instances of the transmission-antenna within the array of the antenna [29].

The constellation points in the three-dimensional field and the pattern point in the signal field are usually plotted in Spatial Modulation for any number of data bits that make up a single unit. At every stance of a single transmission, antennas of the whole set would be activated. Others would have a zero-power transmission. Hence, ICI instituted at the reception point as well as the necessity to harmonize the antennas of the transmitter are entirely circumvented. At the reception point, maximum receive ration combining (MRRC) - which essentially is the highest reception ratio merging - is utilized to approximate the number of antennas for transmission, then the symbol communicated is projected. The two projections are utilized by the three-dimensional demodulator to recover the block-data bits [30]. Antenna embedding results in a hybrid variation of MIMO, where the moderated signals are contained in a three-dimensional constellation map, which combines spatial and signal information.

Figure 2.2 highlights the SM transmission methods based on ON/OFF concept.



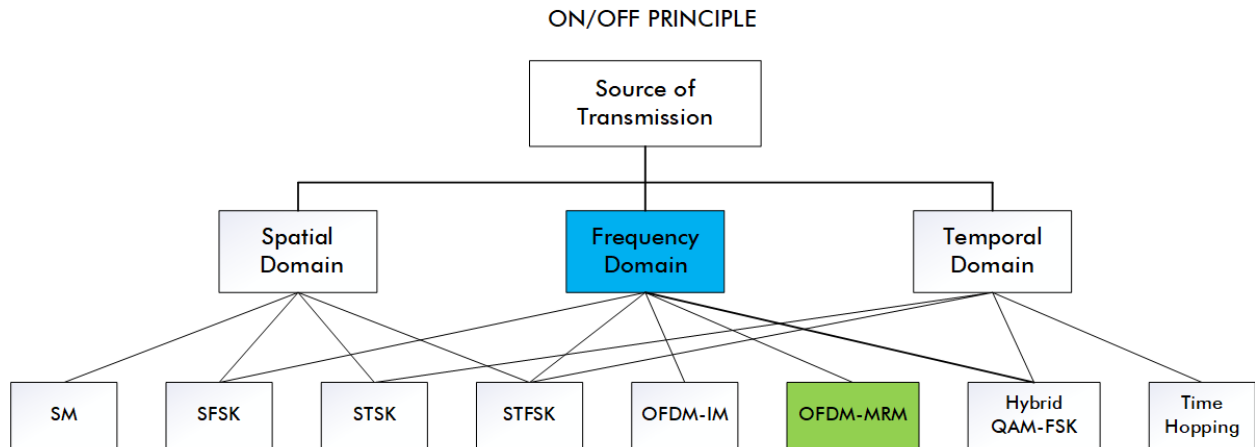


Figure 2.2 - SM Transmission Techniques based on ON/OFF Principle

In Figure 2.3 below, every point of the spatial constellation describes an autonomous complex plane of points of the signal constellation.

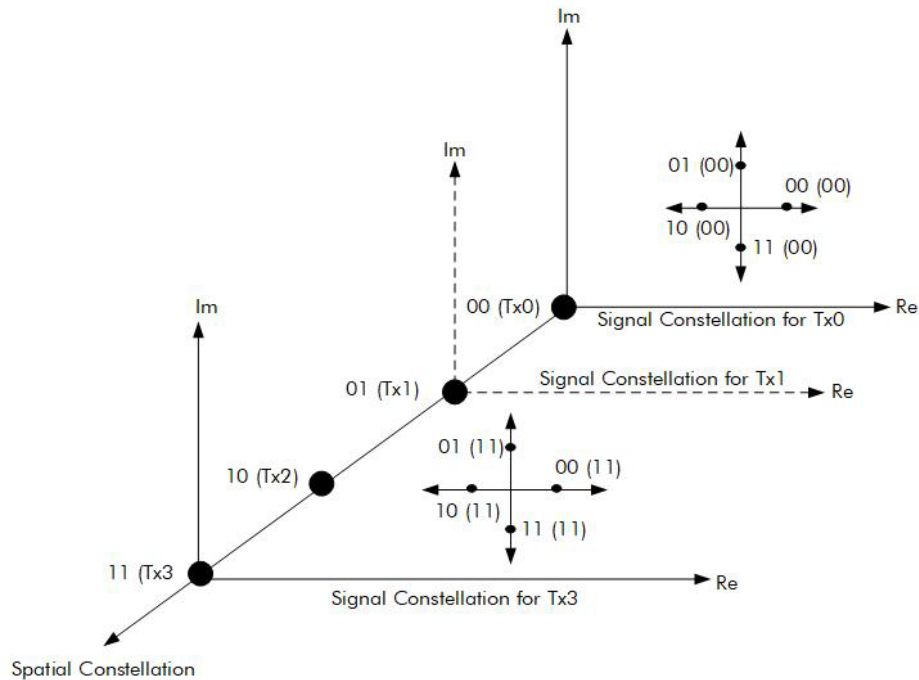


Figure 2.3 – Spatial Modulation constellation diagram in three-dimension

### 2.2.1 SM Transmitter

The division of the bitstream produced by the binary source is carried out in the transmitter. Each block in the bitstream contains  $\log_2(M) + \log_2(N_t)$  bits on every stance, where, the  $\log_2(M)$  and  $\log_2(N_t)$  represent the symbols contained in the diagram of the constellation of signals and the bit numbers required to know the antennas which are transmitting and contained in an array of the antenna respectively. Every block bit is then handled by a locator of SM, as shown in Figure 2.4, which separates them into two distinct sub-blocks of  $\log_2(M)$  and  $\log_2(N_t)$  bits. The bits that make up the first sub-block i.e.,  $\log_2(N_t)$ , helps in the selection of the antenna, which is activated for information communication, whereas all the other transmission-antenna are made silent in the present interval of signaling time. The 2<sup>nd</sup> sub-block i.e.,  $\log_2(M)$ , bits help in choosing a symbol in the diagram of the constellation of the signal. According to Figure 2.4, the activation of transmit antenna two (Tx2) for data transmission will be done by the initial two bits a – 1 and a “10” binary signal, which would be taken out from the following 3<sup>rd</sup> bit (1). In the event that the SSK modulation is considered instead of spatial modulation, each switched on transmit antenna will transmit the same signal out. Hence, the data will be programmed only at the position in the context of the antenna array.

Figure 2.4 depicts a linear receiver cluster with four transmit antennas and a Quadrature Phase Shift Keying (QPSK) modulation i.e.,  $N_t = 4$ . When just the transmit-antenna index is utilized to send data, it becomes an SSK variant that circumvents any kind of traditional variation and trades-off intricacy of the receiver for attainable data rates [31].

Spatial Modulation operability can be broadly categorized into three sections i.e., the Transmitter, Communication Channel and Receiver. This is shown in Figure 2.4 which illustrates how SM works.

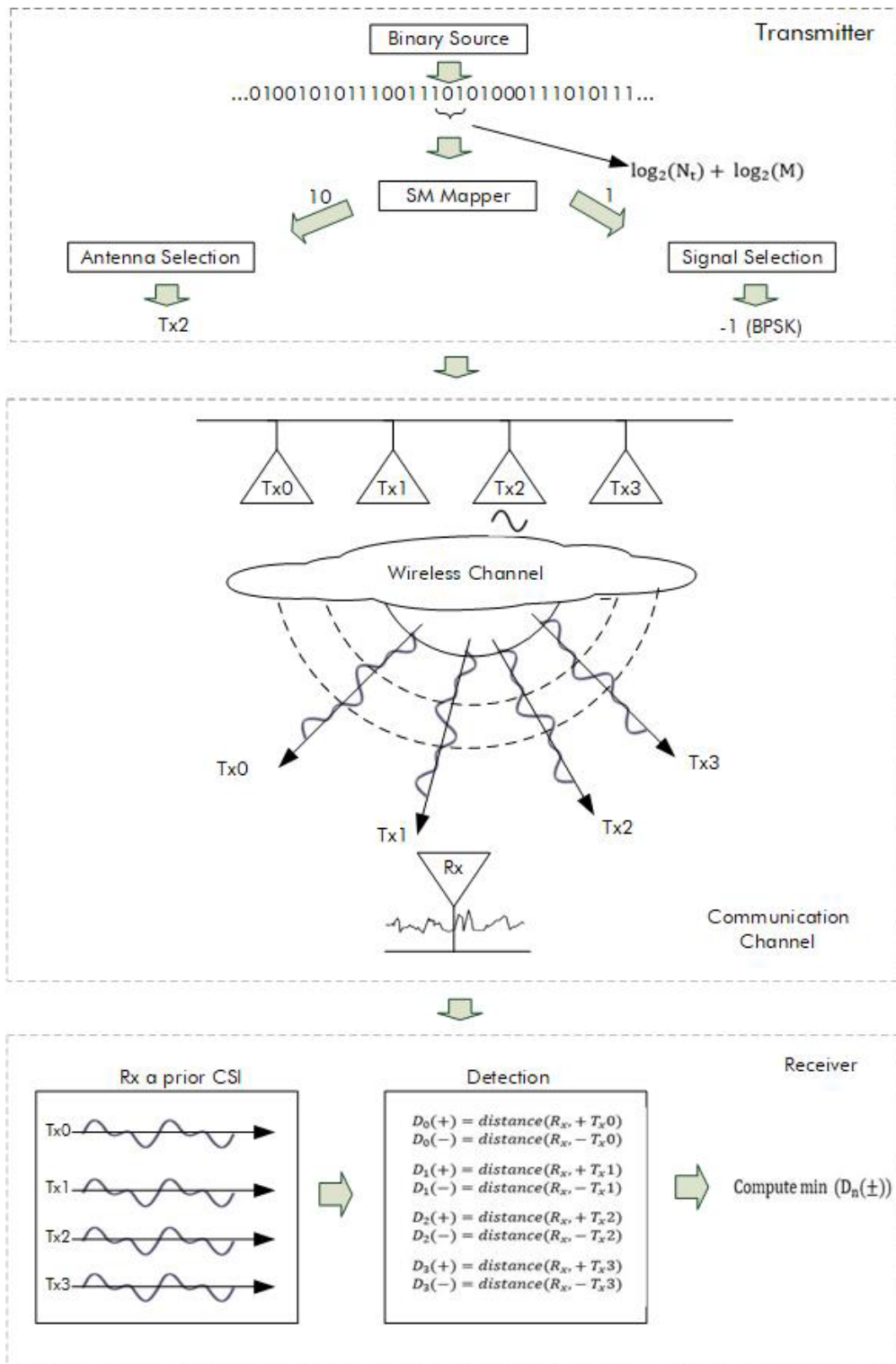


Figure 2.4 - How Spatial Modulation Works

For SM functionality, a mapping table is used. An illustration of this is shown in Table 2.2.

Table 2.2 – S.M Mapping Table

<b>Input Bits</b>	<b>Antenna Number</b>	<b>Transmit Symbol</b>
<b>000</b>	1	-1
<b>001</b>	1	+1
<b>010</b>	2	-1
<b>011</b>	2	+1
<b>100</b>	3	-1
<b>101</b>	3	+1
<b>110</b>	4	-1
<b>111</b>	4	+1

### 2.2.2 SM Channel

The wireless channel of SM acts comparable to a variation unit. The active antenna's signal is then passed through a wireless channel that is generic. Because of the differentials in the spatial positions that are occupied by the antennas that are transmitting in the array of the antenna, the transmitted signal through every antenna is deemed to experience a varied propagation situation because of the different interrelating environmental objects contained along with any wireless link of transmission and reception. This situation represents the basic functioning principle of the spatial modulation that shows the signals interrupting upon a unit receive antenna and conforming to the 4 transmit-antenna as illustrated in Figure 2.4. It should be distinguished that only a unit transmit-antenna is seen to be activated at every period, hence, only a unit signal would be captured. The other projections would radiate no single power. Accordingly, the channel (wireless) is very instrumental in the role of 'modulation unit' through the introduction of a unique thumbprint capable of making the signal emitted by a specific transmit-antenna that is unique at the receiver. In the event that the receive-transmit links (wireless) are not substantially dissimilar, the conveyance of data might not be possible because the emitted signals by the transmission antenna would be apparently similar.

### 2.2.3 SM Receiver

The reception device utilizes the arbitrary variation instituted by the wireless communication network for the recognition of signals. Figure 2.4 outlines a maximum likelihood (ML) detector at the reception with sufficient Channel State Information (CSI) [32]. To recognize the communicated signal emanating from the highly disturbed (noisy) signal receiver (Rx), the reception should notice, through channel approximation, a priori the channel instinct response of all the wireless connections that are transmit-to-receive. In Figure 2.4, the receiver should estimate four responses of channel impulse (which includes receive-filters and the effects of the transmit and) since there is one receive antenna and four transmitting antennas i.e.,  $N_r = 1$  and  $N_t = 4$ . According to the ML principle, the receiver calculates the Euclidean length from the detected signal to the set of potential signals restricted by the wireless channel (which includes signal variance when SM is employed) and selects the nearest one. Generally,  $MN_tN_r$  Euclidean lengths need to be calculated. As a result, all of the bits in the transmitted block could be decrypted, and the original bitstream could be retrieved [32].

The SM operating approach is based on the wireless setting naturally managing the broadcast signal, with each wireless transmit-to-receive link having its own channel, and the receiver using prior channel familiarity to distinguish the signal transmitted. SM utilizes the place-specific feature of the wireless network, - the distinctiveness of each wireless transmit-to-receive connection, for communication and hence varies from SDMA. Variations in network impulse responses are investigated for multiple access in SDMA, but they are not used for data modulation [33].

Before transmitting data symbols via a specific antenna defined by an antenna index, SM may partition data input into numerous antenna indices and data symbols. It should be mentioned, however, that the poorer factor between the data symbol and antenna index performances has a significant impact on its ability to perform. A receiver and transmitter that is more power-efficient based are hence, required to give a different level of protection according to the level of importance of the data as well as, improve on the performance of the receiver compared to the traditional SM. To offer uneven error protection (UEP) at the transmission point, two Forward Error Correction (FEC) codes are employed to encode the data symbol and the antenna

separately. A novel method of two-stage decoding and detection is used at reception to improve the bit error rate [34]. Table 2.3 highlights the advantages and disadvantages of SM.

Table 2.3 - Merits and Demerits of Spatial Modulation (SM)

Merits	Demerits
<ul style="list-style-type: none"> <li>i. SM avoids ICI and IAS completely.</li> <li>ii. To transmit data, only one transmit antenna is turned on, while all other antennas are kept silent.</li> <li>iii. The multiplexing gain increases logarithmically with the number of transmit antennas when using the tridimensionality constellation diagram in SM.</li> <li>iv. SM provides a high-spectral-efficiency code with an equivalent code rate greater than one.</li> <li>v. In contrast to conventional spatial multiplexing methods for MIMO systems, the ICI does not require complicated interference cancellation algorithms, so the receiver design is simple.</li> <li>vi. SM can decode ML using a simple single-stream receiver.</li> <li>vii. When the number of reception antennas is smaller than the number of broadcast antennas, SM can operate efficiently because the receive antennas are used solely for diversity gain.</li> <li>viii. Different transmitter and receiver pairs are usually located in different locations, which makes it possible for SM to be used in multiple-access scenarios.</li> <li>ix. When used in MIMO systems, SM has a higher data capacity than standard low-complexity coding schemes.</li> </ul>	<ul style="list-style-type: none"> <li>i. When using the SM concept, at least two transmit antennas are needed.</li> <li>ii. For wireless links that transmit and receive data and are not sufficiently different, the SM paradigm may not be used, or its performance may fall short of what is expected. It is, however, analogous to the constraints of traditional spatial multiplexing systems, which require a dense scattering environment to ensure a large increase in throughput [35].</li> <li>iii. Receivers need to know the channel perfectly to detect data, which puts a lot of pressure on the channel estimation unit.</li> <li>iv. As the quantum of transmit antennas increases in SM, the data rate increases in a logarithmic manner, not linearly. For practical numbers of antennas at the transmitter, SM may be limited in its ability to achieve very high spectral efficiencies.</li> </ul>

### **2.3 Generalized Spatial Modulation**

In a novel way, generalized spatial modulation overcomes SM's requirement that the number of transmit antenna elements be a power of two. A packet of information bits in GSM is allocated a constellation identifier and a spatial identifier. The space symbol is a collection of broadcast antennas that are always active. The incoming data stream determines the actual configuration of the active transmits antennas. In contrast to the SM, only one transmitting antenna is operational at any given time. When compared to the number of antenna options, GSM boosts total spectral efficiency by two logarithms. As a result, to achieve the same spectral efficiency, fewer transmit antennas are required. GSM functions essentially identically to SM, but with a significantly greater number of transmit antennas [36].

### **2.4 Space Shift Keying**

In SSK, rather than transmission symbols, the employed antenna index during transmission provides information. The required transceiver elements for amplitude/phase modulation transmission and detection are not present because there is no symbol information (such as coherent detectors). Additionally, compared to SM, the simplicity of the modulation reduces the complexity of detection while yielding nearly equal performance benefits. However, the lack of amplitude/phase modulation gives SSK significant differences and advantages over conventional SM, namely, (i) the detection complexity is reduced while the performance is nearly identical to optimal SM detection; (ii) because the criteria for transceivers are less strict than those for amplitude/phase modulation, inconsistent detectors can be considered.; and (iii) SSK's simplicity of framing is advantageous [37].

### **2.5 Generalized Space Shift Keying**

To surpass classic amplitude/phase modulation (APM) approaches in wireless communication, GSSK modulation takes use of fading. In GSSK, rather than the symbols themselves (like in SM and APM), the antenna indices broadcast information. To boost performance, it makes use of GSSK's degrees of freedom. GSSK takes use of the fading process by expanding the dimension of the constellation, resulting in widely separated points, by building its constellation in the best possible method. APM is outperformed by GSSK (up to 5 dB). All of the benefits of SM

discussed in [30] are also available in GSSK (at equivalent performance), but with less computational cost and greater design freedom. GSSK is a good choice for transceivers with reduced complexity in next-generation communication systems because of these advantages [38].

## **2.6 Multiple Active Spatial Modulation**

The multiple active spatial modulation (MASM) technology can achieve equal spectral efficiency to standard SM by using fewer transmit antennas, active RF chains, and receive antennas. When a similar number of transmit antennas are used as in standard SM, MASM achieves higher spectral efficiency and fewer active RF chains and receiver antennas are employed. MASM's adjustable selection of active RF chains generalizes the SM idea and enables more effective tradeoffs between spectrum efficiency, energy efficiency, detection complexity, IAS and ICI. MASM can exceed standard SM approaches in SE performance by employing a lower modulation level, while also improving energy efficiency, detection complexity, and the number of active RF chains and receiver antennas required. This allows MASM to save money on antenna components, the ICI and IAS, implementation complexity, and space and power needs as compared to other SM variations. In addition, an enhanced variant of MASM is presented (E-MASM), which achieves greater SE and energy efficiency rates by providing a better balance between spectral efficiency and variety when compared to SM. When compared to other SM variations and significant space modulation approaches, EMASM is more dependable, although MASM is more efficient in terms of spectrum efficiency [39].

## **2.7 Extended Spatial Modulation**

Extended spatial modulation (ESM) is a spatial modulation technique that employs a variable number of active antennas. As additional symbols become accessible for transmission, data rates may improve, allowing more information bits to be modulated during each time slot. As additional symbols become available for optimization, the minimal distance between transmitted symbols may be increased, boosting symbol error performance even more. Furthermore, it adopts a low-complexity near-optimal detection strategy whose benefits over standard SM may be graphically displayed and utilized to show the efficacy of its suggested detection technique and confirm the theoretical theory [40].



## 2.8 Layered Spatial Modulation

Layered Spatial Modulation (LSM) is a modulation system that can transmit numerous data layers to various users through activating only one transmit antenna. A group of antennas are assigned to a specific user symbol and upon activation of one of the antennas, the user is set to detect a corresponding symbol. As a result, all antennas will be used to transmit data to this end-user. Another user's assigned sets should be distinct from those of other users to create a separation between their data sets. Nonetheless, mutual antennas will exist between two different sets representing two symbols. It is critical that all assigned pair sets have an equal number of shared antennas since if they do not, the pair sets with the most common antennas will have low error performance [41]. LSM combines a power-efficient transmitter and receiver to offer different levels of protection with the goal of providing hierarchical transmission and to enhance the reception performance through the use of UEP which functions on account of unequal detection performances between data symbol and antenna index making it feasible to prevent the degradation performance of the SM system [34].

## 2.9 Subcarrier-Index Modulation

Subcarrier Index Modulation (SIM) takes advantage of subcarrier orthogonality by adding a new dimension known as the subcarrier index dimension (SID) to the already complex and traditional amplitude/phase modulation (APM) techniques such as quadrature amplitude modulation (QAM) and amplitude shift keying (ASK) [42]. The main idea of SIM is to use the subcarrier index to send data in on-off mode. When the SIM is used with OFDM and alternative power allocation rules, such as power saving and reallocation policies, the OFDM SIM enables better BER performance with power advantages and energy efficiency compared to conventional OFDM [42]. The input bitstream is split into two secondary bitstreams of similar size using SIM OFDM [42].

Table 2.4 highlights the merits and demerits of SIM.

Table 2.4 - Merits and Demerits of Subcarrier Index Modulation (SIM) [40]

Merits	Demerits
<ul style="list-style-type: none"> <li>i. When it comes to information transmission, it takes advantage of the orthogonality of the multi-carrier dimension.</li> <li>ii. When PRP is used, the amount of transmit power per subcarrier increases, resulting in better error rate performance than conventional OFDM.</li> <li>iii. SIM OFDM is a suitable choice for energy-efficient systems and green radio applications in light of PSP.</li> <li>iv. More robustness and less inter-subcarrier interference in frequency-selective fade channels.</li> <li>v. The spectral efficiency is improved by using excess subcarriers.</li> <li>vi. Use of existing technology for simple subcarrier status detection (coherent OOK detection).</li> </ul>	<ul style="list-style-type: none"> <li>i. Power efficiency must be traded off to achieve enhanced BER performance.</li> </ul>

## 2.10 Multiple Rank Modulation

Multiple Rank Modulation (MRM) involves the reception at a transmitter, a signal with a range of bits and dividing the signal received into a signal modulation and a rank index bit block. The bit block modulation signal is programmed in a system for further transmission. The rank index bit block helps in selecting a rank to be initiated, in which the activated rank has no less than one activated transmitter projection and the programmed bit block signal modulation is conveyed via the stimulated rank being not less than one initiated antenna for transmission. The conveyed encoded bit block for signal modulation is acknowledged via the receiving antenna and a rank index, a receiver as well as a symbol of transmission projected from the received signal. The bit block signal variation is decoded finally. A system model for MRM is shown in Figure 2.5.

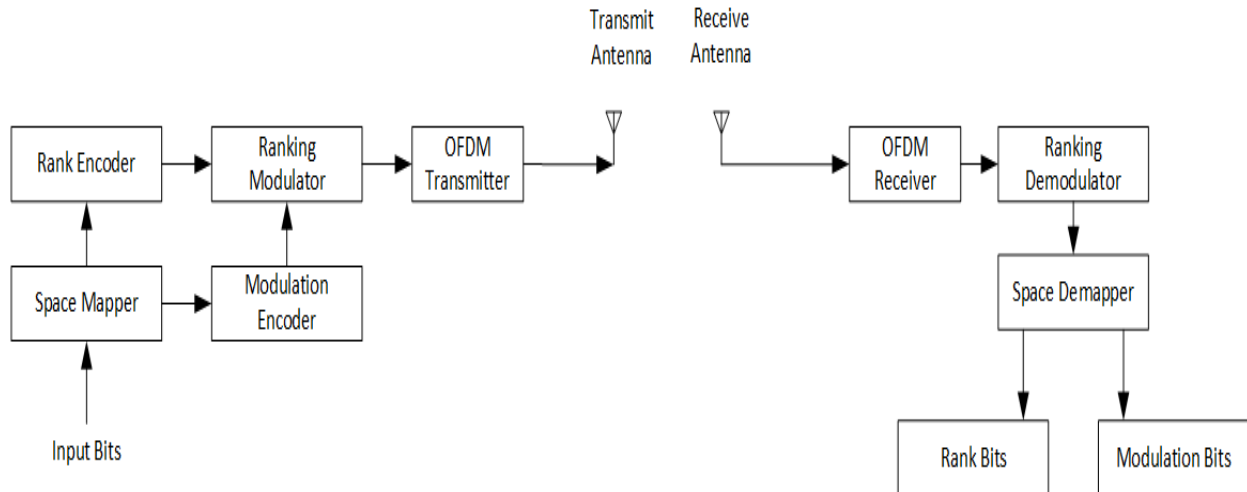


Figure 2.5 - MRM System Model [6]

For the proposed system, the transmission will be done via OFDM. The selected frequencies will have a uniform guard band interval which can be pre-defined. At the side of the receiver, the ML algorithm detection method is used to project the number of frequencies that did transmit the signal and in turn, also calculates the rank that is activated. This has the effect of reducing the receiver complexity in comparison to other algorithms used in traditional MIMO systems.

At the detector side, the rank index and broadcast symbol may be projected from the received signal. The estimated rank index is used by the ranking demodulator to decode the rank bit block, whereas the projected broadcast symbol is used to decode the signal variation bit block. As part of a MIMO system, MRM initiates the transmission of at least one antenna thereby reducing the spatial errors and permitting the inter-channel interference (ICI).

The advantages and demerits of MRM are highlighted in Table 2.5.

Table 2.5 - Merits and Demerits of Multiple rank Modulation (MRM)

Merits	Demerits
<ul style="list-style-type: none"> <li>i. Increased information security is added by the inclusion of a mapping table where various antennas are used to convey information.</li> <li>ii. Reduction in high demodulation complexity and errors in the spatial domain compared to conventional SM.</li> <li>iii. Channel capacity and data rates are increased since MRM relies on the index of a multiple rank active among a plurality of multiple ranks as a data source [2].</li> </ul>	<ul style="list-style-type: none"> <li>i. Each antenna head may require its own RF structure, so the number of RF chains that can be implemented is limited [35].</li> </ul>

### 2.11 Motivation

In recent years, Index Modulation (IM) schemes have received a lot of attention [43-47]. To send more information bits, IM leverages indices associated with building components of linked communication systems [48]. Traditional digital modulation technologies that carry information by modulating a sinusoidal carrier signal are replaced by IM systems [48]. In place of traditional digital modulation techniques, IM systems can be employed. By changing the on/off state of its transmitting parameters, such as transmitting antennas, subcarriers, RF reflectors, modulation types, network slots, precoder networks, broadcast networks, and so on, IM systems basically add additional dimensions to data transmission. In theory, instant messaging could help all forms of communication systems. A new generation of digital modulation techniques arose with the introduction of spatial modulation (SM) and OFDMIM concepts [47]. The possibility of spatial modulation is further explored in this new wave of digital modulation approaches.

Spatial MRM, as described in [6] and [49], uses the number of transmitting antennas per time slot as the source of information for multi-rank modulation (MRM). A similar approach for sequence modulation has been presented in [48], which derives information from frequency, symbols, or antenna sequences. Unlike other IM systems, FMRM uses only a single transmit

antenna and, unlike spatial modulation, thus it is not necessary to use a fading channel to detect subcarriers.

Whereas all other IM schemes have been more fully characterized in literature, the performance of an FMRM scheme is still unknown. This work characterizes FMRM in terms of BER and proposes a simulation framework, detection mechanism and validation framework to be used for FMRM.

## CHAPTER 3: METHODOLOGY

### 3.1 FMRM System Model

The proposed FMRM system model is depicted in Figure 3.1. It is made up of four building blocks i.e. (i) Signal processing block (ii) Channel transmission block (iii) Receive block and (iv) FMRM detector block. The input symbols are fed onto the signal processing unit which processes the input symbols by discarding some symbols of the entire OFDM block and assigns them different frequency indices for transmission. These OFDM symbols to be transmitted are then projected to the transmitting antenna and transmission occurs depending on the selected rank. The transmitted symbols are subsequently routed across the channel, which introduces additive noise, and modulation occurs at this stage. The transmitted signals are then received at the receive antennas in the receive block section where the rank of the transmitted symbols is detected. At the FMRM detector, the received OFDM symbols are then processed using the system mapper and also employs a threshold detector to ascertain the exact input symbols that were transmitted.

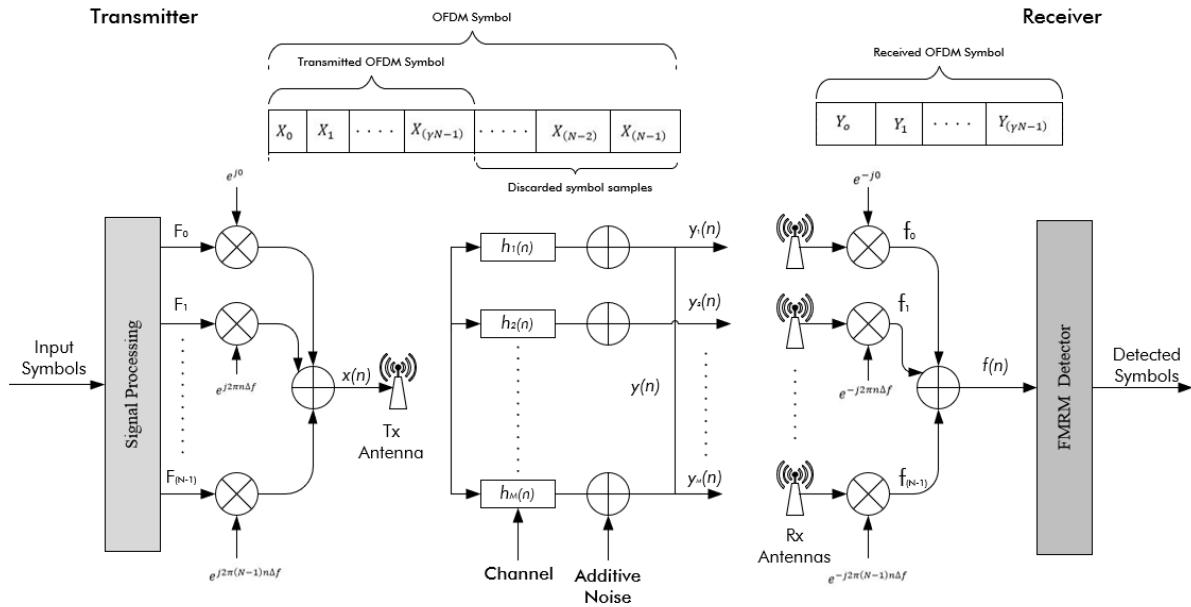


Figure 3.1 – FMRM System Model

### 3.2 Signal Transmission

Using a time truncation factor of  $\tau$ , it is possible to produce an OFDM symbol  $x(t)$  by multiplexing an  $N$  input vector of a complex signal  $F$  onto parallel subcarriers. The frequency spacing between two neighboring subcarriers in truncated OFDM signals is defined as  $\frac{1}{T_{OFDM}}$ , which is similar to the frequency spacing between OFDM signals. Thus, the equation for the sent signal is given as:

$$x(t) = \frac{1}{\sqrt{T_{TOFDM}}} \sum_{l=-\infty}^{\infty} \sum_{n=0}^{N-1} F_{l,n} \exp\left(\frac{j2\pi(t - l\tau T_{OFDM})}{T_{OFDM}}\right) \quad (3.1)$$

where,  $F_{l,n}$  is the modulated data symbol on the  $n^{th}$  subcarrier and  $l^{th}$  OFDM symbol,  $N$  identifies the subcarrier index and  $\frac{1}{\sqrt{T_{TOFDM}}}$  is a normalization factor. When the transmitted OFDM signal is truncated, the resulting truncated OFDM symbol can be calculated.

Taking into account  $T_{TOFDM} = \tau T_{OFDM}$ , Equation 3.1 can be re-written as:

$$x(t) = \frac{1}{\sqrt{T_{TOFDM}}} \sum_{l=-\infty}^{\infty} \sum_{n=0}^{N-1} F_{l,n} \exp\left(\frac{j2\pi(t - lT_{TOFDM})}{T_{OFDM}}\right) \quad (3.2)$$

Because the previous symbol was truncated, the succeeding symbol comes  $(1 - \tau)$  sooner for each truncation. Trimmed OFDM signals are not orthogonal to their OFDM counterparts with greater transmission speeds of each subcarrier because the truncated OFDM symbol duration is not equal to the reciprocal of the frequency spacing between the subcarriers; for example, in the same time slot as eight OFDM signals, 10 truncated OFDM symbols may be broadcast.

Through the use of an OFDM symbol with a sample period of  $\frac{T_{OFDM}}{H}$ , where  $H = \rho N$  and  $\rho \geq 1$  is the oversampling rate, the method of modulating data input onto distinct subcarriers in a discrete truncated OFDM signal is denoted as [50]:

$$X(k) = x \left( \frac{kT_{OFDM}}{H} \right) = \frac{1}{\sqrt{\tau H}} \sum_{n=0}^{H-1} F_n \exp \left( \frac{j2\pi nk}{H} \right) \quad (3.3)$$

where  $k$  is the index of the truncated OFDM time sample for the range  $0 \leq k \leq \tau H - 1$ . In matrix form, Equation 3.3 can be expressed as follows [50]:

$$X = \Phi * F \quad (3.4)$$

$X = [x_0, x_1, \dots, x_{\tau H-1}]^T$  denotes a  $\tau H$ -dimensional vector that is a sampled truncated OFDM symbol in the time domain,  $F = [f_0, f_1, \dots, f_{\tau H-1}]^T$  is an  $N$ -dimensional vector that is a sampled input data in the frequency domain.  $\Phi$  represents a two-dimensional carrier matrix that has been sampled i.e.,  $\tau H \times H$ . The elements of subcarrier matrix  $\Phi$  are given by  $\Phi_{k,n} = \frac{1}{\sqrt{\tau H}} \exp \left( \frac{j2\pi nk}{H} \right)$  where  $0 \leq k \leq H - 1$  and  $0 \leq k \leq \tau H - 1$ .

During the signal transmission process, an Additive White Gaussian (AWGN) noise  $n = [n_1, n_2, \dots, n_{N_r}]^T$  is applied to a modulated signal  $x(t)$ , where  $N_r$  indicates the count of the receive antennas. The signal that is received is provided by:

$$\mathbf{y}(t) = \sqrt{\bar{\gamma}} \mathbf{x} + \mathbf{n} \quad (3.5)$$

where the average signal to noise ratio (SNR) is  $\bar{\gamma}$  at each receive antenna. The noise,  $n$  has the distribution  $\mathcal{CN}(0,1)$ , which has entries that are both independent and identical (i.i.d.) entries. Dissecting the signal component  $x$  of Equation 3.5 gives the equation of a sinusoid i.e.,

$$x = \sin(wt) \quad (3.6)$$

$w$  can be reduced to its most basic form, i.e.,

$$w_i = 2\pi f_i \quad (3.7)$$



Thus, we have Equation 3.5 expounded as:

$$\mathbf{y} = \sqrt{\bar{\gamma}} \left( \sum_i \sin 2\pi f_i t \right) + \mathbf{n} \quad (3.8)$$

As illustrated in (3.8), the focus of this thesis is on the frequency component of the modulated signal, by altering the frequency  $f_i$  during transmission. This causes a particular rank to be activated during transmission, with each rank comprising a certain number of transmitting frequencies, the least of which is one. At the receiver, the frequency MRM detector determines the rank of the bit stream, which is then used to decode the frequency domain supplied input bits.

### 3.2.1 Rician Channel Transmission

A Rician channel presupposes a direct line of sight (LoS) between the transmitter and the receiver. The signal received over a Rician multipath channel, in terms of pdf, can be modelled as:

$$p(r) = \frac{r}{\sigma^2} \exp\left(-\frac{r^2 + s^2}{2\sigma^2}\right) I_0\left(\frac{rs}{\sigma^2}\right) \quad (3.9)$$

where  $s$  is the field strength of the LoS component and  $I_0$  is the first kind zero-order modified Bessel function,  $\sigma$  is the distribution mode and  $r$  is a random variable, which actually represents the magnitude of the complex envelope. The theoretical BER for Rician fading channel using BPSK is given as:

$$\mathbf{P}_b = \frac{1}{2} \operatorname{erfc} \left( \sqrt{\frac{K \left(\frac{E_b}{N_0}\right)}{\left(K + \frac{E_b}{N_0}\right)}} \right) \quad (3.10)$$

where  $K$  is the Rician factor and  $\frac{E_b}{N_0}$  is the SNR per symbol.  $K$  is modelled as  $10$  for this thesis.

When  $K$  is 0, the channel becomes a Rayleigh channel. The received signal is expressed as follows.

$$\mathbf{y} = \sqrt{\bar{\gamma}} \mathbf{h} (\sum_i \sin 2\pi f_i t) + \mathbf{n} \quad (3.11)$$

where  $\mathbf{h}$  is the Rician channel and is represented by  $h = \frac{K\Omega}{K+1}$ .  $\Omega$  is the received signal power.

### 3.3 FMRM Sample Mapper

Table 3.1 below illustrates a sample mapping table for FMRM.

Table 3.1 - Mapping Table for FMRM

Input Bits	Frequency Index (MHz)	Rank
000	$f_1$	1
001	$f_1, f_2$	2
010	$f_1, f_2, f_3$	3
011	$f_1, f_2, f_3, f_4$	4
100	$f_1, f_2, f_3, f_4, f_5$	5
101	$f_1, f_2, f_3, f_4, f_5, f_6$	6
110	$f_1, f_2, f_3, f_4, f_5, f_6, f_7$	7
111	$f_1, f_2, f_3, f_4, f_5, f_6, f_7, f_8$	8

The mapping Table 3.1 demonstrates a sample FMRM mapping method that can be used in the case of three bits per second transmission in each timeslot, activating different ranks depending on the transmitted bit. The points,  $p$ , where the  $n_s$  subcarrier is employed in the OFDM transmission determine the pattern of the  $n_s$  subcarriers. This thesis presents a simple example in which known signals are conveyed.

### 3.4 Signal Detection

#### 3.4.1 Maximum Likelihood (ML)

The FMRM technique is similar to traditional SM in that it detects both the transmit antenna index  $\hat{j}$  and an estimate of the transmitted symbol  $q$ . The maximum probability decision rule is used by the detector, which is thought to contain optimal channel state information, to calculate the bits and rank index, as shown below:

$$\begin{aligned}
 [\hat{j}, \hat{x}_q] &= \operatorname{argmax} p_{\mathbf{Y}}(\mathbf{y} | \mathbf{x}_{jq}, \mathbf{H}) \\
 &= \operatorname{argmin} \left[ \sqrt{\frac{\bar{\gamma}}{\varphi_0}} \|\mathbf{g}_{jq}\|^2 - 2R_e(\mathbf{y}^H \mathbf{g}_{jq}) \right]
 \end{aligned} \tag{3.12}$$

$$= \underset{j, \hat{q}}{\operatorname{argmin}} \left( \|\mathbf{y} - \mathbf{H}_q\|_F^2 \right)$$

where  $\mathbf{g}_{jq} = \mathbf{h}_j x_q$ ,  $j \in [1 : N_t]$  and  $q \in [1 : M]$ . For a single stream SM scenario, the conditional probability density function (pdf) of  $\mathbf{y}$  given  $\mathbf{H}$  and  $\mathbf{x}_{jq}$  is stated as:

$$p_{\mathbf{Y}}(\mathbf{y} | \mathbf{x}_{jq}, \mathbf{H}) = \frac{1}{\pi^{N_r}} \exp \left( - \left\| \mathbf{y} - \sqrt{\frac{\bar{\gamma}}{\varphi_o}} \mathbf{H} \mathbf{x}_{jq} \right\|_F^2 \right) \quad (3.13)$$

Likewise, as with multiple active spatial modulation (MA-SM), we have:

$$P(\mathbf{y} | \mathbf{H}, \mathbf{x}_{jq}) = \frac{1}{\pi^{N_r} \sigma_N^{2N_r}} \exp \left( - \frac{\|\mathbf{y} - \mathbf{H} \mathbf{x}_{jq}\|_F^2}{\sigma_N^2} \right) \quad (3.14)$$

Making reference to Figure 3.1, Fast Fourier Transform is used to decode the transmitted bits once the received signals are identified and demodulated at the receiver (FFT). Because the transmitted symbols are equally likely at the receiver, the identification of the known modulation symbol is achieved using an optimal FMRM detector. The threshold detector is used to determine the absolute magnitude of the frequency signal, and the FFT operation is performed on the received signals,  $Y$ , to produce frequency signals. The vector  $\mathbf{v}$ , which equals the amplitude at each subcarrier, represents the amplitude at each subcarrier:

$$\mathbf{v} = (2 * |Y(f_i)|), \quad i \in [1 : n_s] \quad (3.15)$$

where,  $n_s$  is the total number of subcarriers as shown in the mapping Table 3.1. For the generation of the output subcarrier placements  $\hat{p}$ , a threshold detector is employed to determine if the amplitude at subcarrier  $i$  is greater than the threshold value  $\delta$ .

$$\hat{p} = \min ([v(i) - \delta] > 0) \quad (3.16)$$

The subcarrier locations' output pattern is then utilized to de-map the transmitted data using the mapping table. Because of this, a threshold detector (TD) is the preferable detection method due to:

- i. It offers high detection speed.
- ii. It has low resource requirements.
- iii. It provides a high detection efficiency.

### 3.4.2 Selection Combining (SC)

The antenna with the greatest SNR is chosen and used in subsequent information processing in SC. Putting the analogy into equation form:

$$w_k = \begin{cases} 1 & \gamma_k = \max_n \{\gamma_n\} \\ 0 & \text{otherwise} \end{cases} \quad (3.17)$$

Because the element picked has the highest SNR, the output SNR of the selection diversity technique is given as  $\gamma = \max_n \{\gamma_n\}$ . To investigate such a diversity system, we take into account the possibility of outage, BER, and the resultant rise in SNR.

The outage probability is the likelihood that the output SNR will go below a threshold  $\gamma_s$ , i.e., the SNR of all components will fall below the threshold. Therefore,

$$\gamma = \max_n \{\gamma_n\} \quad (3.18)$$

$$P_{out} = P[\gamma < \gamma_s] = P[\gamma_0, \gamma_2, \dots, \gamma_N < \gamma_s] = \prod_{n=0}^{N-1} P[\gamma < \gamma_s] \quad (3.19)$$

The product statement in Equation 3.19 is correct because the fading at each element is expected to be independent. Using the pdf of  $\gamma_n$ ,

$$\begin{aligned} P[\gamma < \gamma_s] &= \int_0^{\gamma_s} f_{\hat{\gamma}}(\gamma_n) d\gamma_n = \int_0^{\gamma_s} \frac{1}{\hat{\gamma}} e^{-\frac{\gamma_n}{\hat{\gamma}}} d\gamma_n \\ &= \left[ 1 - e^{-\frac{\gamma_n}{\hat{\gamma}}} \right] \end{aligned} \quad (3.20)$$

The output probability thus becomes:

$$P_{out}(\gamma_s) = \left[ 1 - e^{-\frac{\gamma_n}{\hat{\gamma}}} \right]^N \quad (3.21)$$

Based on the Equation 3.21, the likelihood of an outage diminishes exponentially with the number of antennas. The received signals in diversity systems are equalized using a filter  $w_c$  to generate the symbol estimate  $\hat{x}_{0,c}$  with the equalized symbol being written as [53]:

$$\hat{x}_{0,c} = w_c^H \hat{S} = w_c^H \hat{h}x + w_c^H n \quad (3.22)$$

where  $c$  denotes the type of combiner i.e., Equal Gain Combining (EGC), Maximal Ratio Combining (MRC) or SC.

Referencing Figure 3.1, when several receive antennas are put at the receiver, the basic SC technique can be utilized to increase signal dependability. The combiner picks the receiving branch with the highest signal strength in SC mode, such that [51]:

$$v = \max_j (2 * |Y(f_i, j)|); \quad i \in [1: n_s] \quad \& \quad j \in [1: N_r] \quad (3.23)$$

### 3.5 System Performance Analysis

The performance of the system illustrated in Figure 3.1 under AWGN signals is examined in this thesis. Binary Phase Shift Keying (BPSK) modulation is employed for Bit Error Probability (BEP) analysis, in which the binary symbols last for  $T_s$  seconds apiece during transmission and are characterized by the carrier phase, i.e.

$$s_1(t) = A \cos(2\pi f_c t + \phi_i) \quad (3.24)$$

where  $0 \leq t \leq T_s$  for  $i = 1, 2$  and  $f_c$  is the frequency of the carrier. When the bit is zero, the transmit antenna will transmit  $s_1(t)$ , and when the bit is one the transmit antenna will transmit  $s_2(t)$  with the greatest permissible phase difference between the two bits being  $\pi$ . Postulating  $\phi_1 = 0$  and  $\phi_2 = \pi$ , the two signals will thus be:

$$s_1(t) = A \cos(2\pi f_c t), \quad 0 \leq t \leq T_s \quad (3.25a)$$

$$s_2(t) = \cos(2\pi f_c t + \pi) = -A \cos(2\pi f_c t), \quad 0 \leq t \leq T_s \quad (3.25b)$$

Because binary 0 and 1 are separated by a  $180^\circ$  carrier phase shift, BPSK modulated information can traverse farther distances when sent from base or consumer stations. Figure 3.2 shows how up to three bits can be transmitted via BPSK.

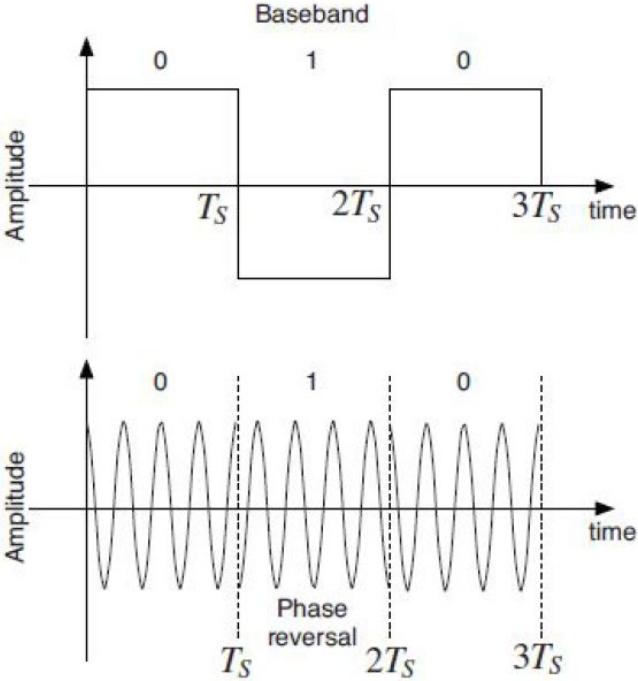


Figure 3.2 – 3Bits BPSK Transmission

### 3.5.1 Bit Error Probability

To characterize the performance of data channels, the bit error rate (BER) is a crucial parameter to consider. The number of errors detected at the receiving end when transmitting data from one point to another such as, over a wireless link or a wired telecommunications link is of utmost importance. It is for this reason that BER/BEP is used to characterize the proposed FMRM system performance.

## 3.5.2 Validation Framework

### 3.5.2.1 Single Receive Antenna

The received signal in Equation 3.5 can be described as follows for a receiver with a single antenna and an AWGN channel with  $h = 1$ :

$$y = x + n \quad (3.26)$$

where  $n \sim \mathcal{CN}(0, \sigma^2)$ ;  $\sigma^2 = N_o$ ;  $x \in (-A, A)$  and SNR,  $\hat{\gamma} = \frac{A}{\sigma^2}$ . Re-writing equation 3.26 using  $n$  as the subject, you get:

$$n = (y - x), n = (y + \sqrt{A}) \quad (3.27)$$

As a result, the probability density function  $P$  can be represented as follows:

$$P = \frac{1}{\sqrt{2\pi\sigma^2}} \exp\left(\frac{-n^2}{2\sigma^2}\right) \quad (3.28)$$

In BPSK, just the true portion of the signal is taken into consideration, where  $N_o = \frac{\sigma^2}{2}$ .

Therefore, the BER for BPSK is given as:

$$P_e = Q\left(\sqrt{\frac{2A}{\sigma^2}}\right) = Q(\sqrt{2\hat{\gamma}}) \quad (3.29)$$

where,  $\hat{\gamma} = \varphi_o \bar{\gamma}$ , is the effective SNR that consists of an oversampling gain  $\varphi_o$  and  $A = \delta$ . The Q function is given by the equation:

$$Q(x) = \frac{1}{\pi} \int_0^{\frac{\pi}{2}} \exp\left(\frac{-x^2}{2\sin^2\theta}\right) d\theta \quad (3.30)$$

Applying the trapezoidal rule to Equation 3.30 yields:

$$Q(x) = \frac{1}{2t} \left( \frac{1}{2} \exp\left(\frac{-x^2}{2}\right) + \sum_{k=1}^{t-1} \exp\left(\frac{-x^2}{S_T}\right) \right) \quad (3.31)$$

where,  $S_T = 2\sin^2\left(\frac{T\pi}{2t}\right)$  and the number of iterations utilized in the approximation is denoted by  $t$ . As a result, the BEP for a system with an AWGN channel is written as [52]:

$$BEP_{AWGN} = \frac{1}{2t} \left( \frac{1}{2} \exp(-\varphi_o \bar{\gamma}) + \sum_{k=1}^{t-1} \exp\left(\frac{-2\varphi_o \bar{\gamma}}{S_T}\right) \right) \quad (3.32)$$

where  $\hat{\gamma}$  is the SNR output branch of the combiner used. To vary the data rates using Equation 3.32, the oversampling gain,  $\varphi_o$ , is varied. Detection of the received signals is then carried out via ML method in accordance with Equations 3.15 and 3.16.

The gain coefficient is important as it enables the data rates to be switched up in the desired manner and at the desired rate. The higher the gain coefficient the faster the switching as well as ability to transfer higher data rates and vice versa.

### 3.5.2.2 Multiple Receive Antennas

When applying diversity at the receiver side with multiple antennas, the BEP is given as by borrowing from the BEP of a single receive antenna (Equation 3.32) and raising it to the power of the number of receive antennas employed:

$$BEP_{AWGN}^d = (BEP_{AWGN})^{N_r} \quad (3.33)$$

For this case, detection of the received signals is then carried out via SC method in accordance with Equation 3.23. Drilling down the case of correlation and diversity for the case of multiple receive antennas, the received signal under correlation is modelled as:

$$y = \hat{h}x + n \quad (3.34)$$



where  $\hat{h} = A * h$ ,  $h$  is the channel impulse response and  $A = Q * \sqrt{D}$ . The values  $Q$  and  $D$  are derived from the Singular Value Decomposition (SVD) of the normalized correlation matrix  $R$  (the factorization of  $R$  into a product of three matrices), where  $Q$  is the position matrix of eigen vectors with orthonormal columns and  $D$  is the diagonal matrix with eigen values with positive real entries.

The correlation matrix  $R$  considers IEEE 802.11n Wi-Fi standard adopted in terms of both frequency and antenna spacing.

### 3.5.2.2.1 Channel Correlation

The system correlation among the antennas is modelled using the conventional method with the correlation coefficient,  $\rho_{kl}$ , between the  $k^{th}$  and  $l^{th}$  antennas branches given as [53]:

$$\rho_{kl} = \frac{E[\hat{h}_k \hat{h}_l]}{\sqrt{\sigma^2_{\hat{h}_k} \sigma^2_{\hat{h}_l}}} \quad l, k = 1, 2, \dots, N_r \quad (3.35)$$

where  $\sigma^2_{\hat{h}_k}$  and  $\sigma^2_{\hat{h}_l}$  denote the variance of the random variables  $\hat{h}_k$  and  $\hat{h}_l$  respectively. The normalized correlation matrix  $R$  is thus given by [53]

$$R = \begin{bmatrix} 1 & \rho_{12} & \cdots & \rho_{1N_r} \\ \rho_{21} & 1 & \cdots & \rho_{2N_r} \\ \vdots & \vdots & 1 & \vdots \\ \rho_{Nr_1} & \cdots & \cdots & 1 \end{bmatrix} \quad (3.36)$$

It is assumed that the formed correlation matrix from Equation 3.36 (i.e., Equation 4.1) is positive definite so that so that it has positive eigen values [54].

Depending on the size of the antenna separation, the signals received by the antennas will be correlated. The correlation model makes the assumption that the linear array of antennas has a uniform angle of arrival distribution. The correlation coefficient, may be calculated using the formula:

$$\rho = J_0 \left[ 2\pi \left( \frac{d}{\lambda} \right) \right] \quad (3.37)$$

where  $J_0(\cdot)$  denotes the zero-order Bessel function of the first kind,  $d$  is the spacing between antennas and  $\lambda$  is the wavelength of the carrier. To obtain the value of lambda we use the formula  $\lambda = \left( \frac{c}{f} \right)$ , with  $c$  denoting speed of light.

## CHAPTER 4: RESULTS AND DISCUSSIONS

Monte Carlo simulations are run to validate the analytical conclusions obtained in the prior sections. Simulation and analytical findings for one-bps, two-bps, and three-bps transmission schemes indicate the system's performance. One transmit antenna and multiple receive antennas are used for the simulations as highlighted in Figure 3.1.

### 4.1 FMRM at Varying Data Rates

Figure 4.1 illustrates that the analytical equation for BER closely matches the simulation findings for all three cases of 1-bps, 2-bps, and 3-bps transmissions. The oversampling gain,  $\varphi_0 = \frac{L/16}{2^{N_s}}$ , where the OFDM length  $L = 1024$ ,  $N_s = 3$  for 1 bit,  $N_s = 5$  for 2 bits and  $N_s = 7$  for 3 bits transmission thus the gain coefficient of oversampling, which is provided by  $\varphi_0$ , is 8, 2, and 0.5 for 1 bps, 2 bps, and 3-bps transmissions, respectively. The gain coefficient limitation is dependent on power.

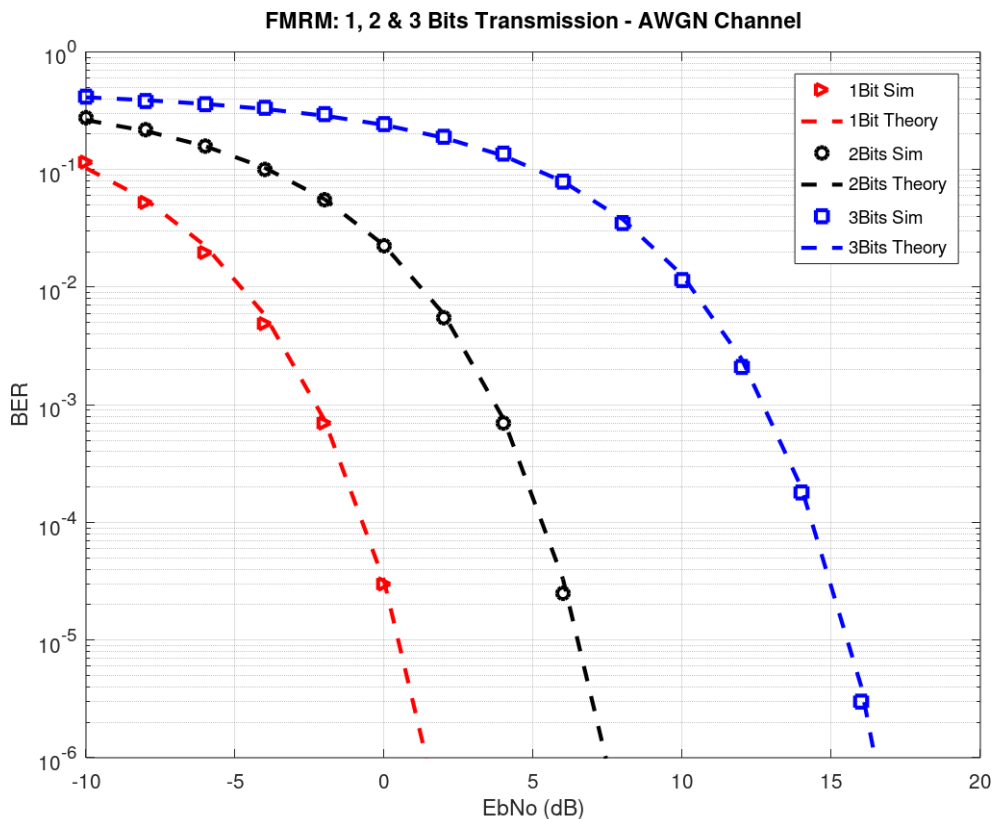


Figure 4.1 – Comparison of FMRM at different data rates

## 4.2 FMRM Comparison with M-QAM

At the same data rates, Figure 4.2 shows a comparison of FMRM and MQAM methods. The oversampling and detection methods used in FMRM are superior to those used in standard MQAM modulation. By roughly 8dB, 1-bps FMRM consumes less power than BPSK. Similarly, 2-bps FMRM uses around 8dB less power than 4QAM. In the case of 3-bps transmission, however, FMRM is just about better than 8QAM because  $\varphi_0 = 0.25$ . This suggests that the detector used in FMRM contributes significantly to decreasing error rates. The detection threshold  $\delta$  is set at 0.6 in these circumstances, at the price of numerous frequencies.

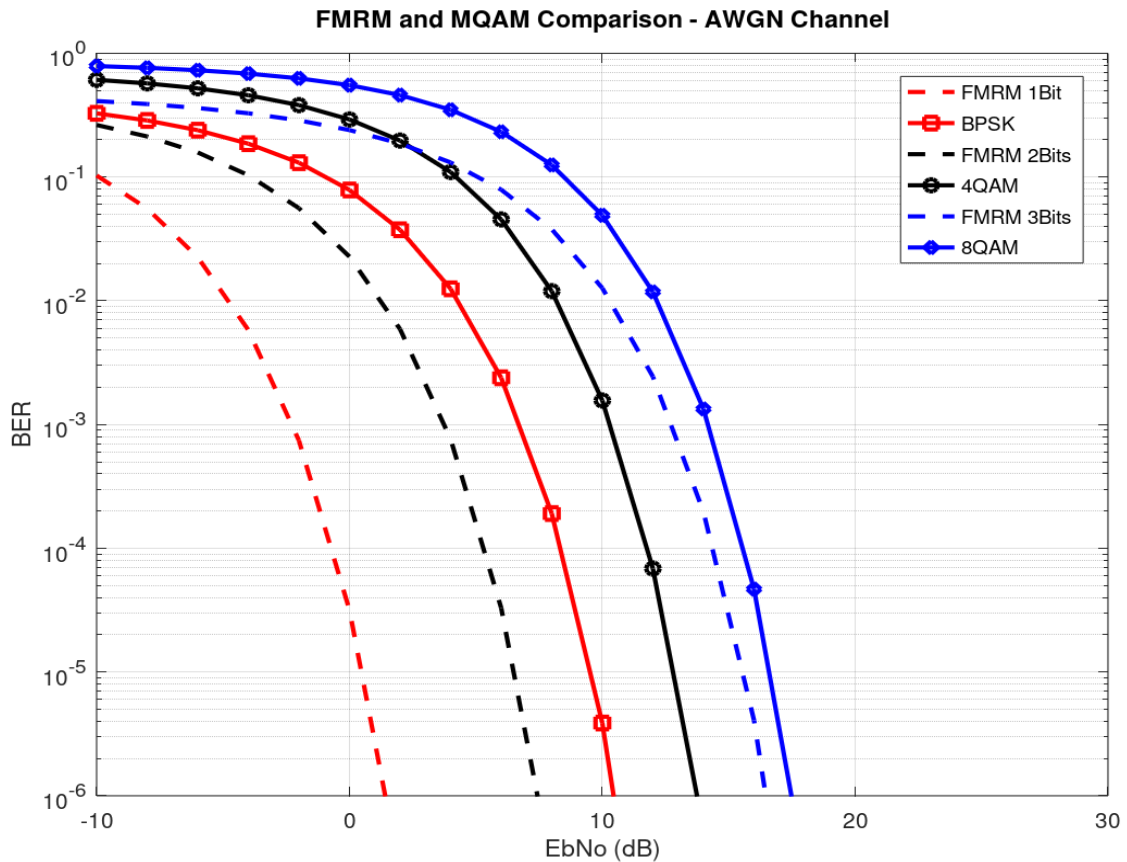


Figure 4.2 - Comparison of FMRM with MQAM

### 4.3 FMRM Comparison with SIM

Figure 4.3 displays a comparison of the FMRM scheme with the Subcarrier Index Modulation (SIM) OFDM system when both data rates are maintained at the same level i.e., 2 bps. In contrast to Subcarrier Index Modulation, it is clear that the oversampling and detection approach used for FMRM is superior to those used for OFDM and SIM OFDM. For the simulations, 50 subcarriers were used for both OFDM and SIM OFDM while 40 subcarriers were used for FMRM simulations. It is clear from the results that the performance of FMRM gets better over conventional OFDM and SIM OFDM as the SNR increases. The SNR deviation between FMRM and SIM OFDM increases from 10.3dB to 11.3dB to 19.5dB and ultimately to 30dB for BER of  $10^{-1}$ ,  $10^{-3}$ ,  $10^{-5}$  and  $10^{-7}$  respectively. On spectral efficiency, OFDM, SIM OFDM and FMRM have a spectral efficiency of 10, 11 and 12.06 [bits/s/Hz] respectively.

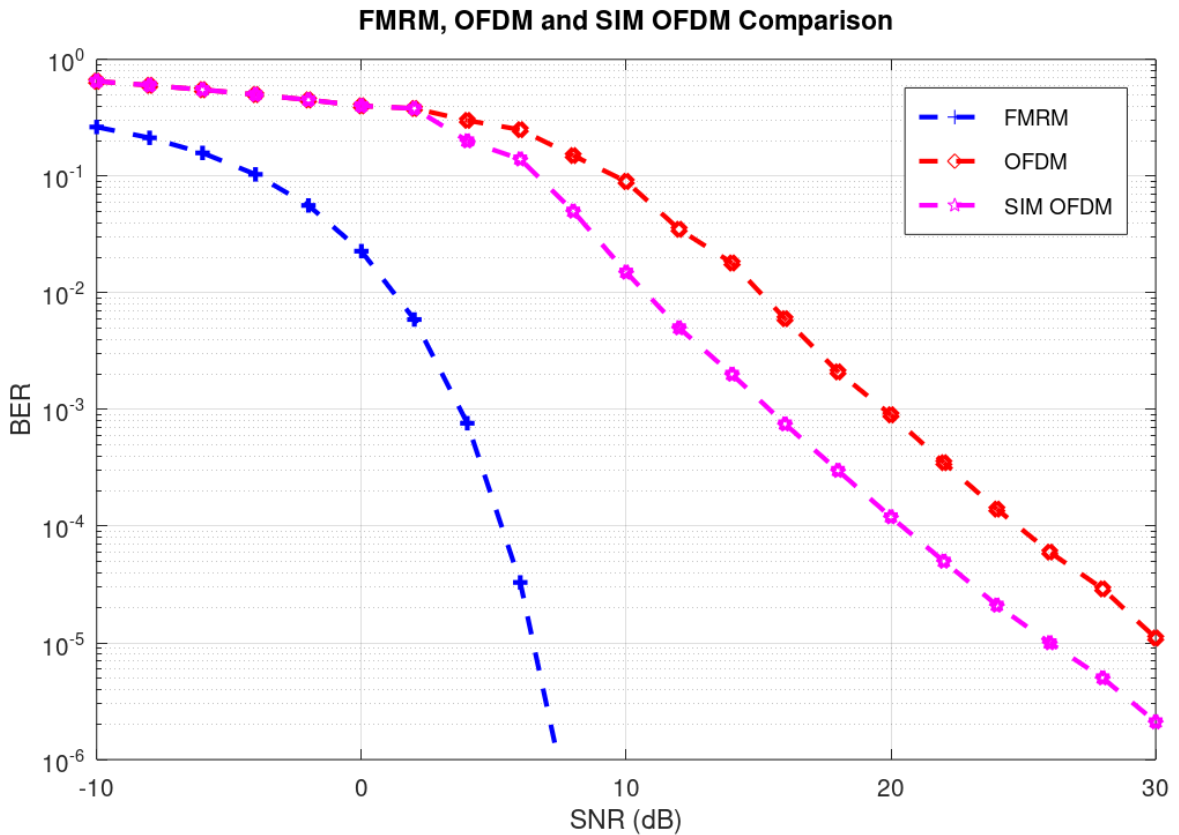


Figure 4.3 – Comparison of FMRM with SIM

#### 4.4 FMRM Threshold Detector

The detector used is dependent on the threshold value  $\delta$ , and as such it is pertinent to give the findings due to the fluctuation of  $\delta$  in order to make a clear comparison. Figure 4.4(a) shows the results for 2-bps transmission when  $\delta$  is varied in the range  $\delta = [0.50 \ 0.55 \ 0.60 \ 0.65 \ 0.70]$ , while Figure 4.4(b) shows the results for 3-bps transmission when  $\delta$  is varied in the range  $\delta = [0.50 \ 0.55 \ 0.60 \ 0.65 \ 0.70]$ . The ideal detection threshold value is 0.6, since it is confirmed by the theoretical framework and yields predicted results from theory. Only by increasing the transmission power can the detection threshold be raised. However, because the goal of every system is to preserve energy, the 0.6 threshold value is chosen for an AWGN channel.

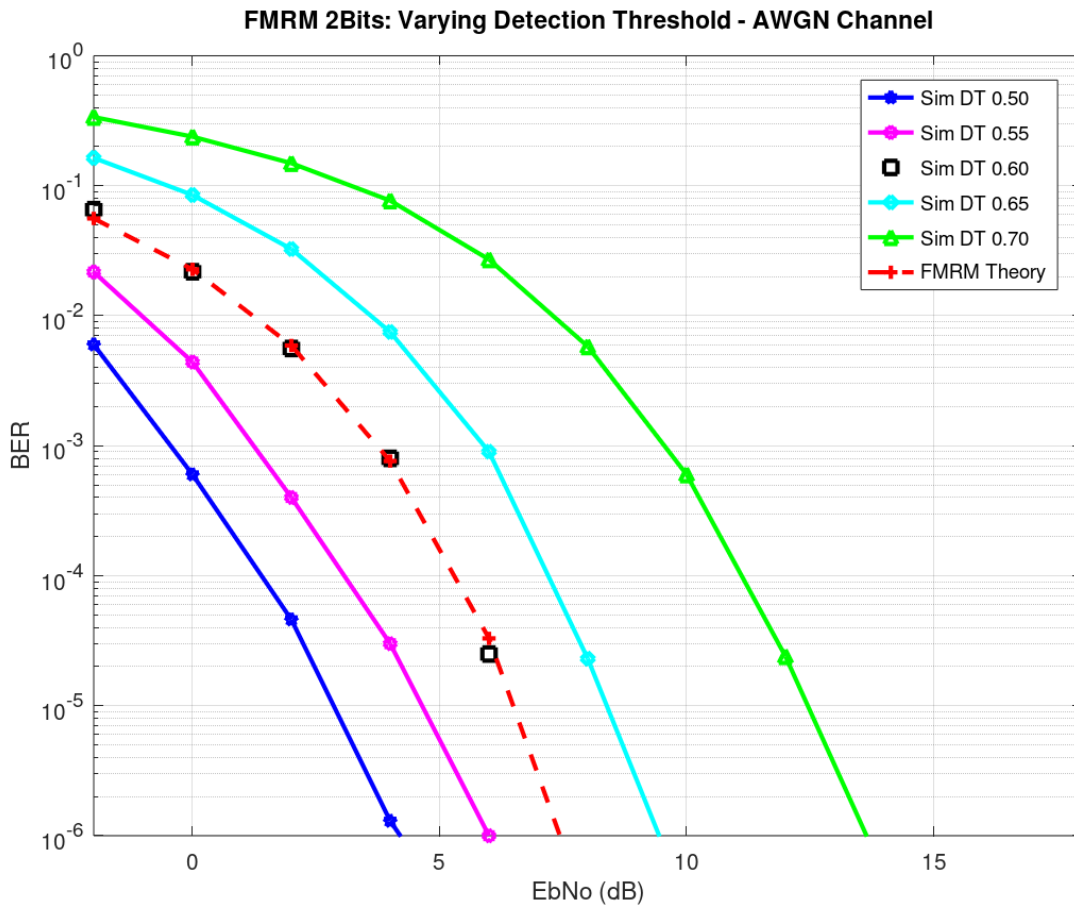


Figure 4.4(a) – Varying FMRM Threshold Detection: 2Bits Tx

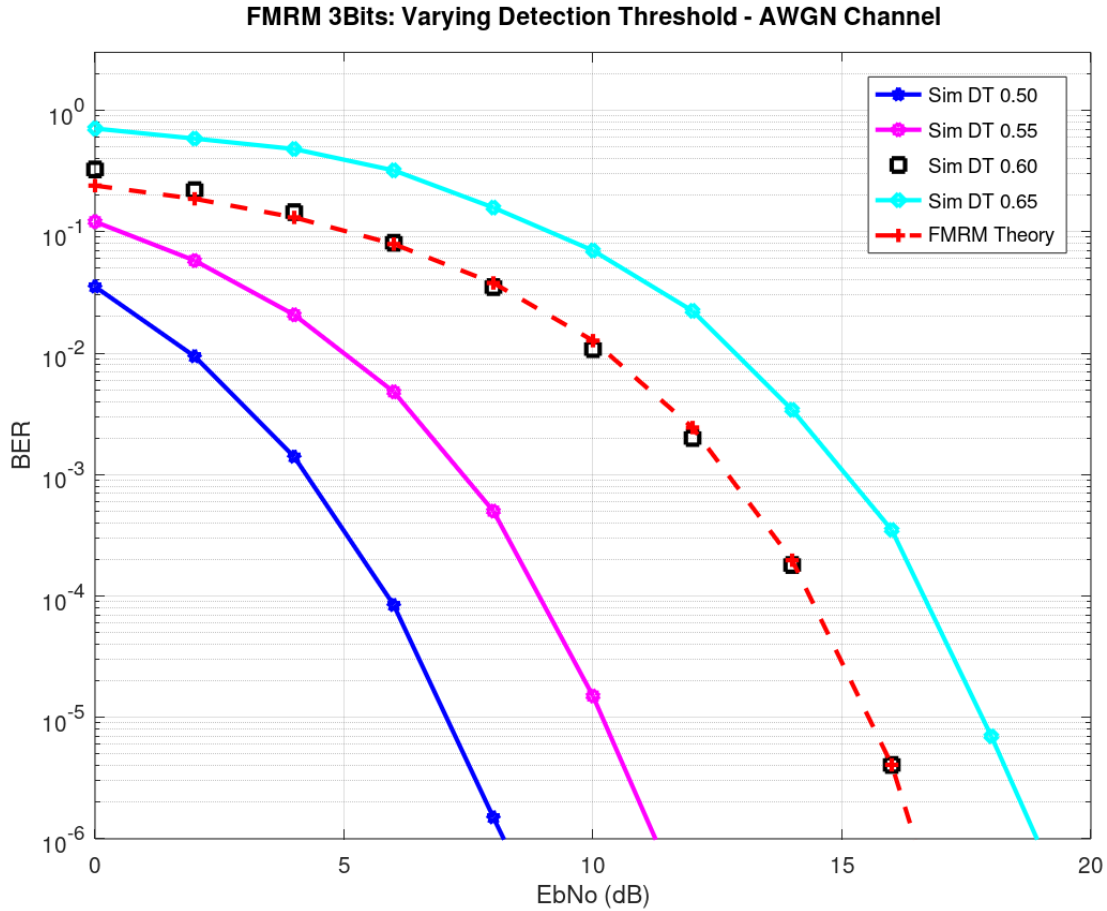


Figure 4.4(b) - Varying FMRM Threshold Detection: 3Bits Tx

#### 4.5 FMRM with SC Diversity

Figures 4.5(a) and 4.5(b) illustrate BER values for different receive antennas at different data rates, i.e., 3bps and 2bps, which are used in receive diversity. To choose the branch with the highest signal strength, a SC combiner is employed. The results demonstrate that the FMRM system works with a SC architecture and that the BER reduces as the quantity of receive branches increases. Furthermore, the simulation results substantially resemble the theoretical conclusions provided and discussed in this thesis. The number of receive antennas is depicted graphically in Figures 4.5(a) and 4.5(b) and denoted as  $N_r$ .

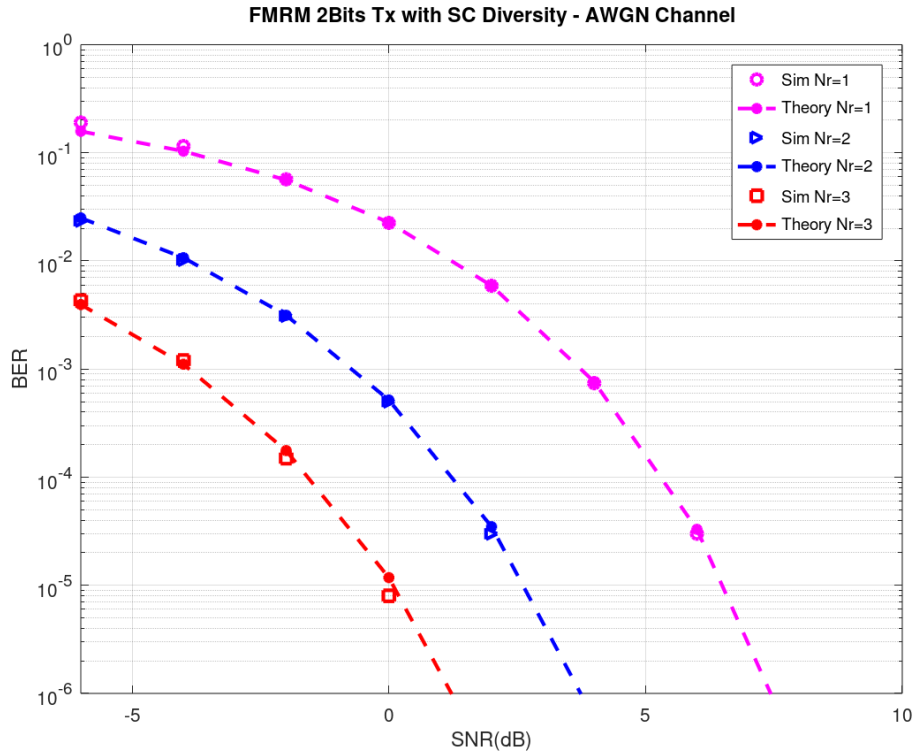


Figure 4.5(a) - FMRM with SC Diversity: 2Bits Tx

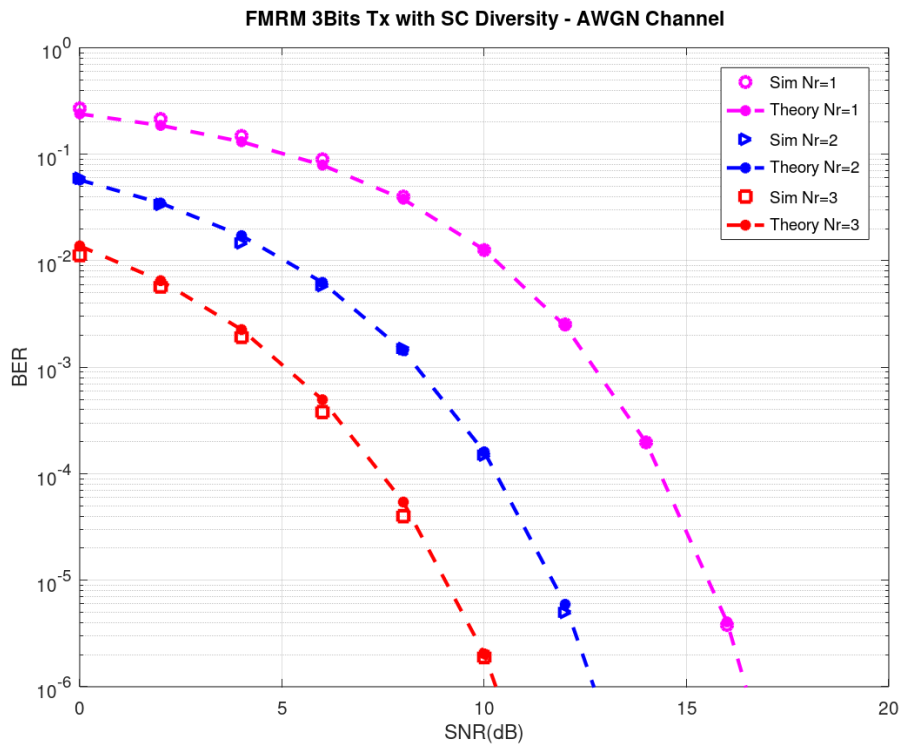


Figure 4.5(b) - FMRM with SC Diversity: 3Bits Tx



#### 4.6 FMRM with SC Diversity and Antenna Correlation

Figures 4.6(a) and 4.6(b) shows BER results for different receive antennas at different data rates i.e., 2bps and 3bps respectively, which are used in the situation of receive diversity coupled with antenna correlation. An antenna correlation spacing of 0.1cm with a wavelength of 0.06m are used for the simulations i.e.,  $d = 0.1\text{cm}$  and  $\lambda = 0.06\text{m}$ , as the values depict real life applications of antennas spacing in devices. Based on these parameters, and using Equation 3.36 and Equation 3.37, the normalized positive-definite correlation matrix  $\mathbf{R}$  consisting of different correlation coefficients for four equally spaced receive antennas is given as:

$$\mathbf{R} = \begin{bmatrix} 1 & 0.99726 & 0.98906 \\ 0.99726 & 1 & 0.99726 \\ 0.98906 & 0.99726 & 1 \end{bmatrix} \quad (4.1)$$

To model the correlation at the receive antennas ( $R_x$ ), for the case of  $N_r = 1$ , only one antenna is considered to receive the signal i.e., either antenna one, two or three. For the case of  $N_r = 2$ , two antennas are considered to receive the signal with the receiving antennas correlated in pairs i.e., antenna one correlated against antenna two or antenna one correlated against antenna three or antenna two correlated against antenna three. For the case of  $N_r = 3$ , all the three antennas are considered to receive the signal and are correlated against each other i.e., antenna one correlated against antennas two and three or antenna two correlated against antennas one and three or antenna three correlated against antennas one and two.

The branch with the highest signal power is then chosen using an SC combiner, which takes into account the correlation between the antennas in the setup. The obtained results show that the FMRM system is consistent with such an SC design when the correlation is taken into account, and that the BER reduces as the number of receive branches increases as compared to their corresponding antennas when a correlation is not taken into account. For both the 2bps and 3bps transmissions, there is a 4dB shift in BER between the two situations (correlation and no correlation). Furthermore, in the situation of antenna correlation, the simulation findings closely match the expected theoretical results.

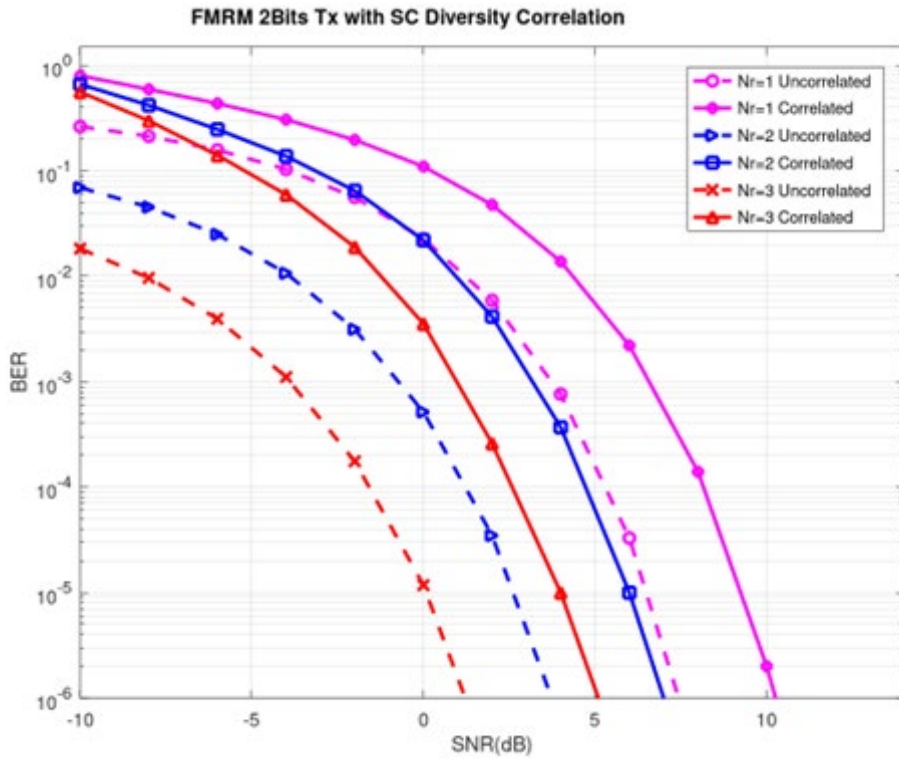


Figure 4.6(a) - FMRM with SC Diversity and Antenna Correlation: 2Bits Tx

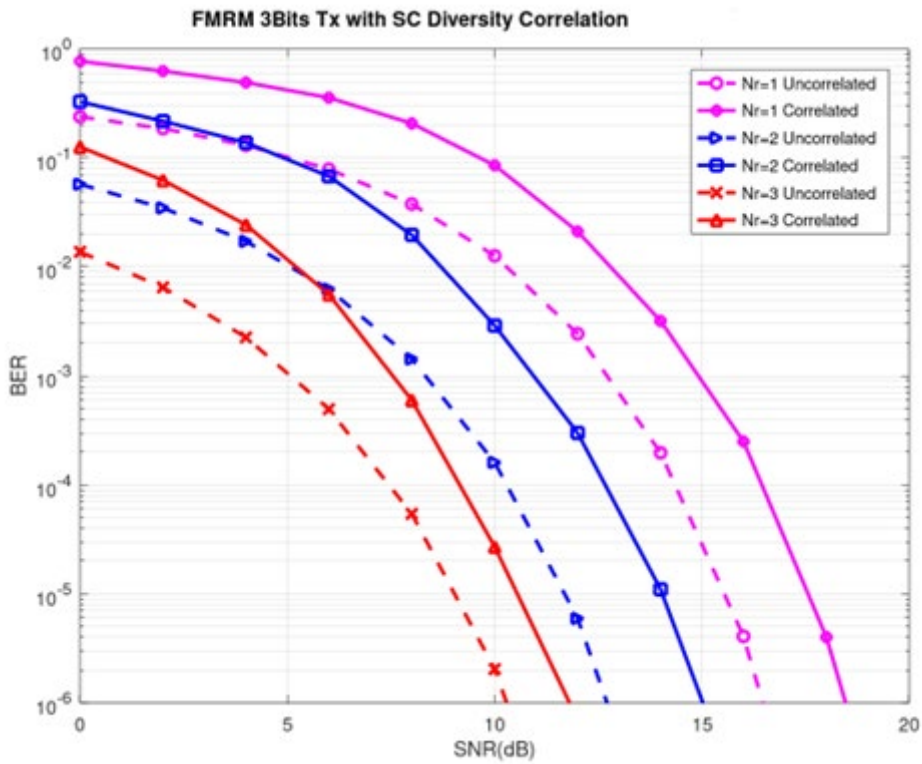


Figure 4.6(b) - FMRM with SC Diversity and Antenna Correlation: 3Bits Tx

#### 4.7 FMRM at Varying Data Rates - Rician Channel

Figure 4.7 shows BER results for the FMRM system when modelled under a flat fading Rician channel. Here, it can be observed that there is an increase in the BER for the different data rates transmission. For the case of 1bps transmission, there is a deviation of 4dB at BER  $10^{-1}$  to 3dB at BER  $10^{-6}$  between the AWGN and Rician channels. For the case of 2bps transmission, there is a deviation of 4dB at BER  $10^{-1}$  to 3dB at BER  $10^{-6}$  between the AWGN and Rician channels. For the case of 3bps transmission, there is a deviation of 4dB at BER  $10^{-1}$  to 2dB at BER  $10^{-6}$  between the AWGN and Rician channels. With this, it can be observed that as the data rates increase, the BER likewise rises with an increase in SNR. The system can thus be said to perform as expected in the flat-fading Rician channel i.e., increase in BER as the channel conditions deteriorate.

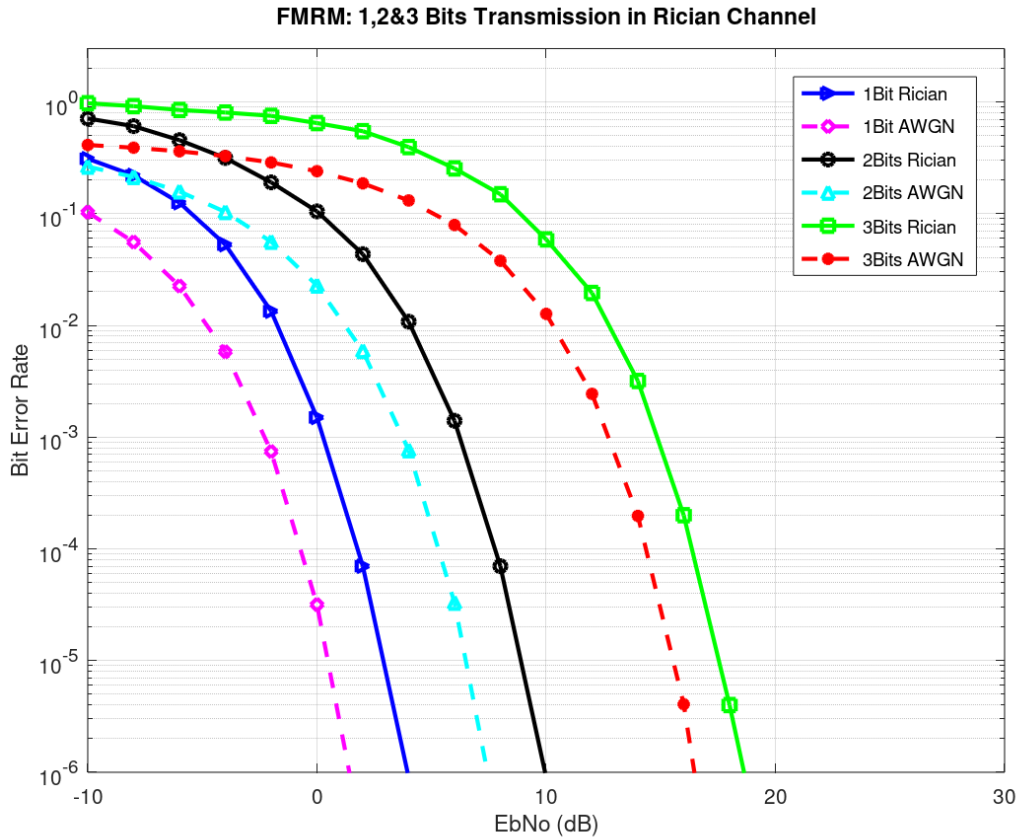


Figure 4.7 – Comparison of FMRM at different data rates: Rician Channel

### 4.8 FMRM Threshold Detector - Rician Channel

Because the detector used is dependent on the threshold value  $\delta$ , it is required to give the findings due to the fluctuation in order to make a clear comparison. For the instance of 1-bps transmission, Figure 4.8 displays the results when  $\delta$  is varied in the range  $\delta = [0.20 \ 0.25 \ 0.30 \ 0.35 \ 0.40]$ . The ideal detection threshold value is 0.3, as this is the one that is supported by the theoretical framework and produces predicted results. This can be seen as a drop in value of 0.3 points from the threshold value of 0.6 earlier on discussed in section 4.2 for the case of AWGN channel as a result of the Rician channel conditions (line of sight) which necessitate the need to lower the detection threshold value if the power level used is to be maintained constant for the same system, albeit different channel conditions.

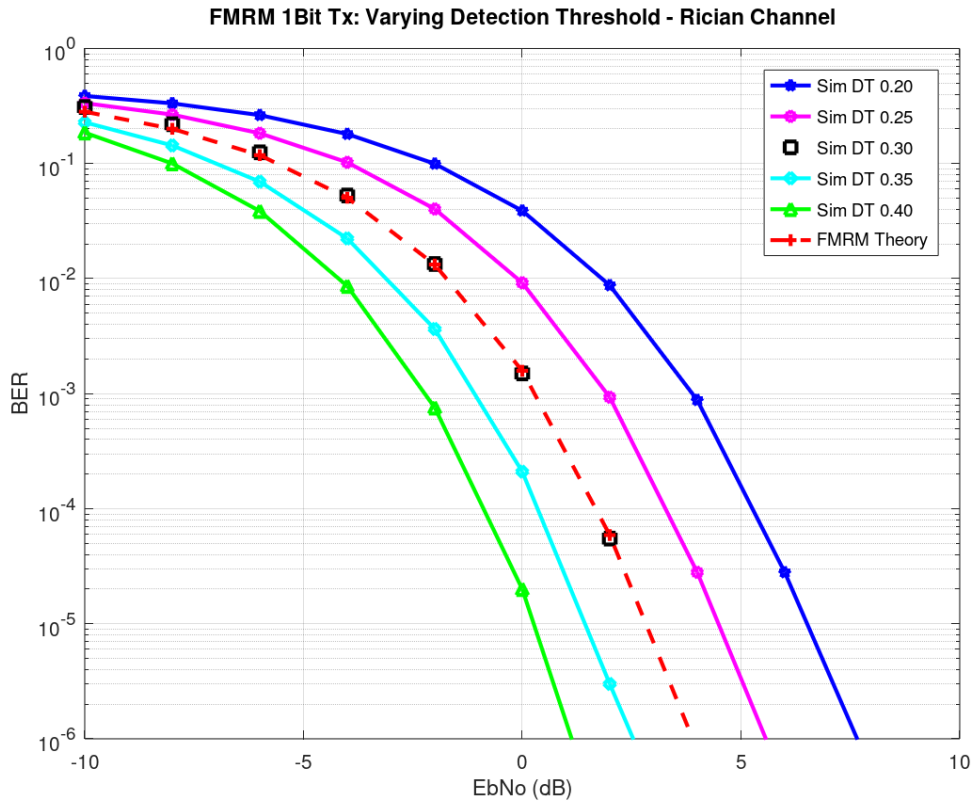


Figure 4.8 – Varying FMRM Threshold Detection: Rician Channel

Referencing Equation 3.10 and modifying the same to obtain the BER for FMRM under Rician fading channel yields the below equation used to obtain the values in Figure 4.8 above:

$$P_b = 0.5 * \operatorname{erfc} \left( \sqrt{\left(10^{\left(\frac{\bar{\gamma}}{10}\right)}\right) * \left(\frac{L/16}{2^{N_s}}\right)} \right) \quad (4.2)$$

where  $\bar{\gamma}$  represents the average SNR per symbol and is given as  $\bar{\gamma} = \Omega \frac{E_b}{N_0}$  with  $\Omega = \varepsilon \langle |h|^2 \rangle$  being average fading power,  $N_s$  the number of subcarriers and  $L$  the length of the OFDM symbol.

For this case, a threshold valued of  $\delta = 0.3$  is preferred over a value of  $\delta = 0.6$  at the same parameters. This is because, to achieve the same value of  $\delta = 0.6$  as is the case of an AWGN channel, the power level for signal transmission has to be increased in order to match this i.e.,  $\Omega$ . However, because the goal of a system is to conserve power as well, the  $\delta = 0.3$  threshold value is the preferable threshold for the system when operating in a flat-fading Rician channel environment at similar operating conditions as the AWGN channel.

## CHAPTER 5: CONCLUSION AND RECOMMENDATIONS

As a final chapter, the findings are summarized based on the scope covered and make recommendations made for any future work that may be undertaken.

### 5.1 Conclusion

The simulation results shown in Chapter 4 have comprehensively characterized the FMRM system performance as set forth in the main objective. Further, these have been validated by the theoretical framework discussed in Chapter 3.

On Reliability investigation and performance analysis on the FMRM system, this has clearly been demonstrated by varying the transmission data rates from 1 bps to 3 bps and simulations done. These have conformed to the expected system behaviour, and they have been validated by the theoretical framework developed in Chapter 3. The results obtained are consistent for every transmission interval and as such the system can be said to be reliable in achieving the objective set. The results for this are clearly shown in Figure 4.1. Further, the data rates have been compared against the conventional transmission schemes at equal data rates i.e., 1-bps transmission has been compared with BPSK, two bps transmission compared with 4-QAM, and 3 bps transmission compared with 8-QAM. From this comparison, FMRM is seen to have a 9 dB gain when compared with BPSK, a 6 dB gain when compared with 4-QAM and a 1 dB gain when compared with 8-QAM. This is illustrated in Figure 4.2. From these, it can be deduced that in terms of BER, the FMRM performs better than the corresponding transmission schemes with matching dates thus clearly showing the performance analysis of the FMRM system. Figure 4.3 further illustrates this by comparing FMRM against conventional OFDM and its enhancement SIM OFDM and being able to achieve gains of up to 30dB.

To achieve the second specific objective of the development of a detection system for the FMRM system brought about by the FMRM bandwidth efficiency being low, the absolute amplitude of the received frequency signals is taken and then the values are compared against the centre frequency values of the transmitted signals. An average of the transmitted centre frequencies is then obtained, and this is used to determine the most suitable threshold value for the threshold system employed in the threshold detector. This is then sampled for different

transmission data rates i.e., 2 bps and 3 bps. From this, the threshold value is seen to be 0.6 for an AWGN channel. This is illustrated in Figures 4.3 and 4.4 respectively.

For the third specific objective on Selection Combining Diversity and Correlation tests using multiple receive antennas using FMRM, this was achieved using receiving antennas with different numbers i.e., from one to three. Furthermore, different data rates were used to test for the selection combining diversity technique and the obtained results conformed to what was expected (theoretical and simulation results matched). Different transmission data rates were also used to validate if the diversity technique (SC) would still hold and indeed it performed as expected as illustrated by Figures 4.5 and 4.6 depicting the case of 2 bps and 3 bps transmission respectively. To add to the diversity objective, antenna correlation tests were also carried out at the receive side using multiple antennas and it was established that whenever there was no correlation at the receive antennas, a gain of 4dB was made for 2 bps transmission and a gain of 2 dB for 3 bps transmission. This is evidenced by Figures 4.7 and 4.8 respectively.

The final specific objective on Performance analysis of the FMRM system in a flat-fading channel, the system was modelled in a flat-fading Rician channel, and the results obtained analysed at different data rates of transmission i.e., 1-bps, 2-bps and 3-bps. It is clearly seen that for the case of 1-bps transmission, the system performance deteriorates in the Rician channel by about 2 dB. However, for 2-bps and 3-bps transmission, this quickly changes, and the system performs better in the fading channel thus highlighting its applicable use even when channel conditions aren't favourable to yield desirable rates suitable for a communication system. This is shown in Figure 4.9. Further, a threshold detector is developed to suit the fading conditions of the Rician channel and through that, a suitable threshold value is obtained (0.3) which allows for the results to be obtained as illustrated by Figure 4.10.

The foregoing explanation of how all the criteria have been accomplished leads to the conclusion that an FMRM communication system has been described that provides adjustable data rates for index modulation systems while remaining cost-effective. Furthermore, it has been proved that the findings of the simulations and the results of the suggested analytical framework are consistent. Because of this, the FMRM system may be used to offset the limits of standard

MRM, particularly when dealing with shifting data rates. In addition, it has been proved that FMRM provides greater flexibility in terms of boosting dependability over standard BPSK and M-QAM at equal data rates and that the addition of the information mapper provides physical layer security advantages.

Table 5.1 - Merits and Demerits of FMRM

Advantages	Disadvantages
<ul style="list-style-type: none"> <li>i. The information sent via the wireless channel is not completely modulated, but the number of frequency chains also modulates the amount of information. This improves the system's reliability to convey information sent.</li> <li>ii. Improves information security operations compared to SIM as it involves the introduction of an information mapper/mapping table, without whose knowledge information cannot be decoded at the receiver.</li> <li>iii. Improved data rates/Better BER performance over comparable schemes with similar data rates e.g., SIM, conventional BPSK, and M-QAM.</li> </ul>	<ul style="list-style-type: none"> <li>i. Low bandwidth efficiency since it requires several subcarriers.</li> </ul>



## 5.2 Recommendations

In a bid to work within the defined scope as well as time constraint factors, this thesis could not comprehensively address all the unreported but identified gaps. As a result, we recommend the following for further/future works. These include but are not limited to:

- Carrying out FMRM system performance analysis over flat-fading Rayleigh channel.
- Conducting further tests for FMRM on flat-fading Rician Channel.
- Using other types of combining e.g., Maximal Ratio Combining (MRC) and Equal Gain Combining (EGC) during signal detection.
- Employing the use of different kinds of threshold detectors (other than ML) during the signal reception.
- Applying antenna correlation during detection using MRC and EGC schemes.

## REFERENCES

- [1] B. Revathi<sup>1</sup>, P.Poonguzhali, A.Angelin, C.Arunachalaperumal, “*The Performance of Spatial Modulation for MIMO Communication*,” IJAREEIE Volume 3, Issue 3npp. 7669-7674, March 2014.
- [2] Khwandah, S.A., Cosmas, J.P., Lazaridis, P.I. et al., “*Massive MIMO Systems for 5G Communications*,” Wireless Pers Commun 120, 2101–2115 (2021).
- [3] Canadian Association for Theatre Research, “*Discussion on the frame structure design for NR*,” 3GPP T Docs TSG RAN WG1, Busan, Korea, Tech. Rep. R1–163132, April 2016.
- [4] J. Chen, M. L. Xu, B. Feng, and Q. G. Tian, “*A novel positioning stage using piezoelectric actuator for antenna pointing*,” Recent Advances in Structural Integrity Analysis - Proceedings of the International Congress, Pages 437-441, 2014 (APCF/SIF-2014).
- [5] G. del Campo, I. Gomez, G. Cañada, L. Piovano, and A. Santamaria, “*Guidelines and criteria for selecting the optimal low-power wide-area network technology*,” LPWAN Technologies for IoT and M2M Applications, Pages 281-305, 2020.
- [6] P.Akuon and H. Xu, “*A Multiple Rank Modulation System*,” SA 2015, US Patent 2018/0269944 A1, 2018.
- [7] X. Cheng, M. Zhang, M. Wen, and L. Yang, “*Index modulation for 5G: Striving to do more with less*,” IEEE Wireless Commun. Mag., vol. 25, no. 2, pp. 126–132, Apr. 2018.
- [8] Q. Li, M. Wen, B. Clerckx, S. Mumtaz, A. Al-Dulaimi and R. Q. Hu, “*Subcarrier Index Modulation for Future Wireless Networks: Principles, Applications, and Challenges*,” March 2020.
- [9] J. Samuel, A. Emmanuel, I. Frank, N. Charles, A. Bayonle, “*Modeling of Orthogonal Frequency Division Multiplexing (OFDM) for Transmission in Broadband Wireless Communications*,” Journal of Emerging Trends in Computing and Information Sciences, Vol. 3, No. 4, April 2012.
- [10] S. J. Vaughan-Nichols, “*OFDM: Back to the Wireless Future*,” IEEE Computer, pp. 19–21, vol.35, issue 12, Dec. 2002.
- [11] Steepest Ascent Ltd., “*The DSPedia (www.steepestascent.com)*,” last access Nov. 2011.

- [12] M. Serra, J. Ordiex, P. Marti and J. Carrabina, “*OFDM Demonstrator: Transmitter,*” in Proc 7th International OFDM Workshop 2002, Sep 2002.
- [13] Ma. J. Canet, F. Vicedo, J. Valls and V. Almenar, “*Design of a Digital Front-End Transmitter For OFDM-WLAN Systems Using FPGA,*” Control, Communications and Signal Processing 2004, First International Symposium on, pp: 503– 506, 2004.
- [14] C. Dick and F. Harris, “*FPGA Implementation of an OFDM PHY,*” Signals, Systems and Computers, 2003. Conference Record of the Thirty-Seventh Asilomar Conference, Vol.1, pp: 905–909, Nov. 2003.
- [15] L. de Souza, P. Ryan, J. Crawford, K. Wong, G. Zyner and T. McDermott, “*Rapid Prototyping of 802.11 wireless modems,*” Solid-State Circuits Conference, 2001. Digest of Technical Papers. ISSCC 2001 IEEE International, pp: 339-495, Feb.2001.
- [16] Y. Kim, H. Jung, H. Ho Lee and K. Rok Cho and F. Harris, “*MAC Implementation for IEEE 802.11 Wireless LAN,*” ATM (ICATM 2001) and High-Speed Intelligent Internet Symposium, 2001. Joint 4th IEEE International Conference on, pp. 192–195, Apr. 2001.
- [17] Y. Awad, L. H. Crockett and R. W. Stewart, "*OFDM transceiver for IEEE 802.20 standards,*" 2009 17th European Signal Processing Conference, 2009, pp. 1-5.
- [18] P. G. Lin, "*OFDM simulation in MATLAB,*" a senior project, Faculty of California Polytechnic State University, San Luis Obispo, June 2010.
- [19] O. Grigoriadis, H. S. Kamath, "*BER Calculation Using Matlab Simulation for OFDM Transmission,*" International Multiconference of Engineers of Computer Scientists (IMECS), vol. II, ISBN. 978-988-17012-1-3, 19-21 March 2008.
- [20] S. B. Weinstein and P.M. Ebert, “*Data transmission by frequency division multiplexing using the discrete Fourier transform,*” IEEE Transactions on Communication Technology”, vol. COM-19, pp. 628-634, October 1971.
- [21] B. Ballal, A. Chadha, N. Satam, “*Orthogonal Frequency Division Multiplexing and its Applications,*” International Journal of Science and Research (IJSR), Volume 2 Issue 1, pp. 325-328, January 2013.
- [22] A. Peled and A. Ruiz, “*Frequency Domain Data Transmission using Reduced Computational Complexity Algorithms,*” In Proc. IEEE Int. Conf. Acoust., Speech, Signal Processing, pp 964-967, Denver, CO, 1980.

- [23] F. M. Gutierrez, P. L. Gilabert, "*Implementation of a Tx/Rx OFDM system in a FPGA*," Master thesis, Francisco Martin Gutierrez, April 30th, 2009.
- [24] K. A. Kadiran, "*Design and implementation of OFDM transmitter and receiver on FPGA hardware*," Master thesis, Universiti Teknologi Malaysia, 10 November 2005.
- [25] M. Helaoui, S. Boumaiza, A. Ghazel, and F. M. Ghannouchi, "*On the RF/DSP design for efficiency of OFDM transmitters*," IEEE Trans. Microw. Theory and Tech., vol. 53, no. 7, pp. 2355-2361, Jul. 2005.
- [26] Z. Sun, X. Liu, and Z. Ji, "*The Design of Radix-4 FFT by FPGA*," International Symposium on Intelligent Information Technology Application Workshops, 2008, pp.765-768.
- [27] A. Cortés, I. Vélez, I. Zalbide, A. Irizar, and J. F. Sevillano, "*An FFT Core for DVB-T/DVB-H Receivers*," VLSI Design, vol. 2008, Article ID 610420, 9-pages , 2008.
- [28] Datasheet. September 2008, "*Xilinx LogiCore Fast Fourier Transform*," Version 4.1, Xilinx Inc. Available: <http://www.xilinx.com>.
- [29] M. Di Renzo, H. Hass, P. Grant, "*Spatial Modulation for Multiple-Antenna Wireless Systems: A Survey*," IEEE Communications Magazine, Volume 49, Issue 12, December 2011.
- [30] R. Mesleh, H. Haas, C.W. Ahn, S. Yun, "*Spatial Modulation*," IEEE Transactions on Vehicular Technology, Vol. 57, No. 4, July 2008.
- [31] J. Jeganathan et al., "*Space Shift Keying Modulation for MIMO Channels*," IEEE Trans. Wireless Commun., vol. 8, no. 7, July 2009, pp. 3692–703.
- [32] J. Jeganathan, A. Ghrayeb, and L. Szczecinski, "*Spatial modulation: Optimal detection and performance analysis*," IEEE Commun. Lett., vol. 12, no. 8, Aug. 2008, pp. 545–47
- [33] J. Mietzner et al., "*Multiple-Antenna Techniques for Wireless Communications — A Comprehensive Literature Survey*," IEEE Commun. Surveys Tut., vol. 11, no. 2, 2nd Quarter 2009, pp. 87–105.
- [34] S. Hwang, S. Jeony, J. Choi, J. Seo, "*A layered spatial modulation technique for MIMO-OFDM systems*," IEEE International Symposium on Broadband Multimedia Systems and Broadcasting (BMSB) 2010.

- [35] J. Mietzner, R. Schober, L. Lampe, W. H. Gerstacker, and P. A. Hoeher, “*Multiple-antenna techniques for wireless communications – A comprehensive literature survey*,” IEEE Commun. Surveys Tuts., vol. 11, no. 2, pp. 87–105, 2nd quarter 2009.
- [36] A. Younis, N. Serafimovski, R. Mesleh and H. Haas, “*Generalised spatial modulation*,” 2010 Conference Record of the Forty Fourth Asilomar Conference on Signals, Systems and Computers.
- [37] J. Jeganathan, A. Ghrayeb, L. Szczecinski and A. Ceron, “*Space shift keying modulation for MIMO channels*,” IEEE Transactions on Wireless Communications ( Volume: 8, Issue: 7, July 2009), pp. 3692–3703.
- [38] J. Jeganathan, A. Ghrayeb, and L. Szczecinski, “*Generalized space shift keying modulation for MIMO channels*,” 2008 IEEE 19th International Symposium on Personal, Indoor and Mobile Radio Communications.
- [39] M. Irfan and S. Aissa, “*Multiple Active Spatial Modulation: A Possibility of More Than Spatial Multiplexing*,” IEEE Wireless Communications Letters ( Volume: 9, Issue: 3, March 2020), pp. 294–297.
- [40] L. He, J. Wang, and J. Song, “*Extended spatial modulation scheme with low complexity detection algorithms*,” 2014 International Wireless Communications and Mobile Computing Conference (IWCMC), pp. 545–47.
- [41] M. Maleki, H. Bahrami, A. Alizadeh, “*Layered Spatial Modulation for Multiuser Communications*,” IEEE Transactions on Wireless Communications, Vol. 15, No. 10, October 2016.
- [42] R. Abu-alhiga and H. Haas, “*Subcarrier-Index Modulation OFDM*,” IEEE 20<sup>th</sup> International Symposium on Personal, Indoor and Mobile Radio Communications, PIMRC 2009, 13-16 September 2009, Tokyo, Japan.
- [43] R. Mesleh, H. Haas, C. Ahn, and S. Yun, “*Spatial modulation- a new low complexity spectral efficiency-enhancing technique*,” First International Conference on Communications and Networking in China (ChinaCom’06), pp.1-5, Oct. 2006.
- [44] E. Basar, “*Index modulation techniques for 5G wireless networks*,” IEEE Commun. Mag., vol. 54, no. 7, pp. 168–175, June 2016.
- [45] H. Haas and M. Di Renzo, “*Enhanced spatial modulation*,” U.S. Patent 20130058390, Feb. 23, 2010.

- [46] P. Akuon and H. Xu, “*Polar coded spatial modulation*,” IET Communications Journal, Volume 8, Issue 9, p. 1459 - 1466, June 2014.
- [47] E. Basar, U. Aygolu, E. Panayirci, and H. V. Poor, “*Orthogonal frequency division multiplexing with index modulation*,” IEEE Trans. Signal Process., vol. 61, no. 22, pp. 5536–5549, Nov. 2013.
- [48] P. Akuon and A. Mwangi, “*Systems and Methods for Communication*,” Publication No. WO/2018/083601, Patent Scope WIPO Grant Number 11258491, February 2022..
- [49] A. Nyawade, P. Akuon and H. Xu, “*Spatial MIMO Rank Modulation*,” IEEE Africon, Accra, Ghana, 2019.
- [50] S. Isam and I. Darwazeh, “*Characterizing the intercarrier interference of non-orthogonal Spectrally Efficient FDM system*,” Communication Systems, Networks and Digital Signal Processing (CSNDSP), 2012 8<sup>th</sup> International Symposium on, Poznan, 2012, pp. 1-5.
- [51] P. Akuon and H. Xu, “*Optimal error analysis of receive diversity schemes on arbitrarily correlated Rayleigh fading channels*,” IET Communications Journal., ISSN 1751-8628, Volume 10, Issue 7, p. 854 – 861, May 2016.
- [52] P. Akuon and H. Xu, “*Performance of multiple active-spatial modulation: information-theoretic criteria over correlated Rayleigh fading channels*,” IET Communications Journal., ISSN 1751-8628, Volume 10, Issue 9, p. 1071 – 1079, June 2016.
- [53] D. G. Brennan, “*Linear diversity combining techniques*,” in *Proceedings of the IEEE*, vol. 91, no. 2, pp. 331-356, Feb. 2003, doi: 10.1109/JPROC.2002.808163.
- [54] Horn, R.A., Johnson, C.R.: “*Matrix Analysis*”, Cambridge University Press, Cambridge, UK, 1990.

## APPENDICES

### Appendix A – Author’s Publications

#### A1. IEEE AFRICON 2021 (Arusha, Tanzania)

# BER Performance of Frequency-coded Multiple Rank Modulation

Jack O. Nyanjom  
School of Engineering  
University of Nairobi  
Nairobi, Kenya  
jack.nyanjom@gmail.com

Peter O. Akuon  
School of Engineering  
University of Nairobi  
Nairobi, Kenya  
akuon@uonbi.ac.ke

Vitalice K. Oduol  
School of Engineering  
University of Nairobi  
Nairobi, Kenya  
vkoduol@uonbi.ac.ke

**Abstract**—A signal transmission technique is proposed where different ranks of frequency subcarriers are used to convey information to the receiver i.e. Frequency-coded Multiple Rank Modulation (FMRM). In FMRM, the number of the subcarriers is determined by the input stream of information bits. The input information bit stream, which is random, is sent into the ranking modulator. Instead of detecting the channel index, the receiver detects the number of frequency subcarriers of an Orthogonal Frequency Division Multiplexing (OFDM) scheme. The pattern of frequency subcarriers is pre-set and known at the receiver using the system mapper. Only the rank information is used to decode the bits in the frequency domain. Analytical upper bounds on Bit Error Probability (BEP) of the FMRM system are derived and then compared with simulation results for different transmission schemes at similar data rates, which show tractable performance. In addition to improved data rates, for better information security operations, the FMRM system has the additional benefit that the wireless channel does not completely modulate the information sent, but the information is also modulated by the number of frequency chains.

**Index Terms**—OFDM, threshold detector, multiple rank modulation

#### I. INTRODUCTION

The basis for the multiple-input multiple-output (MIMO) concept is to increase data rates and reliability by exploiting simultaneous transmission of different signals. High spectral efficiency and reliability can be achieved through spatial multiplexing or spatial diversity like Vertical Bell Labs Layered Space-Time (VBLAST) architecture. However, these schemes suffer from high inter-channel interference (ICI) and they require inter-antenna synchronization (IAS) to avoid inter-symbol interference (ISI). In addition, the detection algorithms at the receiver for MIMO systems have high complexity and the number of receive antennas is required to be equal to or more than the number of transmit antennas. For practical MIMO schemes to be achieved, some trade-offs are essential. Antenna selection schemes, asynchronous transmission and spatial modulation (SM) present admirable trade-offs for conventional MIMO schemes [1-2].

SM is an inventive technique that conveys some information to the receiver based on the spatial signature of the received signal. The spatial signature in SM is provided by the transmit antenna and when the transmit antenna information is detected at the receiver then the spatial information is decoded. This

is possible because it is the spatial information that selects the active transmit antenna. In the conventional SM, only one modulation symbol is transmitted to the receiver by one active transmit antenna per symbol period. Then, both the modulation symbol and the transmit antenna are jointly detected at the receiver. Furthermore, spatial information alone can be utilized to transmit information to the receiver. Such a system has been presented as space-shift keying modulation (SSK) in [3,4].

However, the following concerns can be assessed further in SM systems. The spectral efficiency (SE) of SM increases logarithmically with the number of transmit antennas  $N_t$  i.e.  $SE = \log_2 MN_t$ , where M denotes the modulation index. Therefore, the data rates in SM are lower than VBLAST. Also, the number of transmit antennas is required to be a power of two and thus needs a large number of antennas. However, fractional bit encoded SM (FB-SM), generalized spatial modulation (GSM) and generalized space shift keying (GSSK) can be used to reduce the number of transmit antennas [4]. Furthermore, the wireless channel is the spatial modulator in SM and the detection process may lead to error in the spatial domain in the case where the channels are similar. To this end, power detection has been proposed in the patent of enhanced spatial modulation (ESM) [4]. In ESM, the transmit element is detected using the knowledge of the power allocated at the transmitter to decode the spatial bits i.e. the location of the active transmitter element is detected using the knowledge of the power allocated to the transmitter elements. Similarly, in polar coded spatial modulation (PCSM), the channel rate or the number of bits in the frozen set can be used to relay spatial information to the receiver without encountering any channel errors [5].

#### A. Motivation and Contributions

There has been a tremendous interest in Index Modulation (IM) schemes over the past few years [2-6]. IM is a highly spectrum and energy efficient yet simple digital modulation technique, which utilizes the indices of the building blocks of the corresponding communication systems to convey additional information bits [9]. IM systems provide alternative ways to transmit information in contrast to traditional digital modulation schemes that rely on the modulation of the amplitude/phase/frequency of a sinusoidal carrier signal for

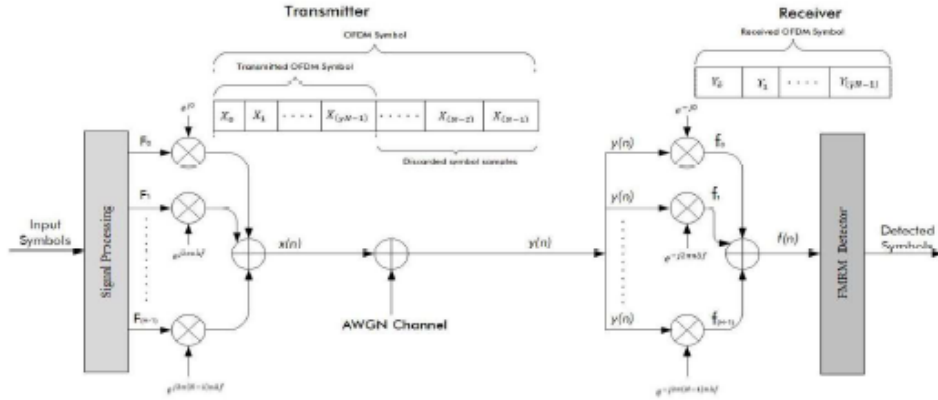


Fig. 1. FMRM System Model

transmission. Radically, IM schemes create completely new dimensions for data transmission by having the ability to map information bits by altering the on/off status of their transmission entities such as transmit antennas, sub carriers, RF mirrors, modulation types, time slots, precoder matrices, dispersion matrices etc. Every communication system can be theoretically considered as a special case of IM. Although early attempts have been made to explore the potential of IM-based schemes after the introduction of spatial modulation (SM) and orthogonal frequency division multiplexing with index modulation (OFDM-IM) concepts by the inspiring works of [6], a new wave of alternative digital modulation schemes has started.

Multiple Rank Modulation (MRM) scheme was proposed in [7] and the spatial MRM is discussed in [8] where the number of transmit antennas used per timeslot is exploited as the source of information. A similar sequence modulation scheme has been proposed in [9], where frequency, symbol or antenna sequences are used as the source of information.

Unlike most IM schemes, the advantage of FMRM is that only a single transmit antenna may be used for transmission, and this saves hardware costs significantly. Furthermore, FMRM does not require a fading channel to distinguish the subcarriers.

### B. Organisation

The rest of this paper is organized as follows: Section 2 introduces the system model and the system mapper, signal transmission scheme and the detection framework at the receiver. Section 3, presents performance analysis of the system based on bit error probability. Section 4 validates the analytical framework with simulation results, while considering non-fading AWGN channel conditions. The paper is then concluded in Section 5.

### C. Notation

Bold upper case symbols denote matrices, while regular letters represent scalar quantities. Bold lower case symbols denote vectors. We use  $\lfloor \cdot \rfloor$  to denote the floor operation,  $(\cdot)!$  to denote the factorial operation and  $E[\cdot]$  to denote the expectation operator.  $\|\cdot\|_F$  denotes the Frobenius norm operator,  $(\cdot)^H$  denotes the Hermitian operator,  $(\cdot)^*$  denotes the conjugate operation and  $(\cdot)^T$  denotes the transpose operation.

## II. SYSTEM MODEL

Figure 1 illustrates the FMRM system model used for this paper. At the transmit side, a truncated OFDM symbol  $x(t)$  is generated by multiplexing a vector of  $N$  inputs of a complex signal  $F$  onto parallel sub-carriers with a time truncation factor  $\tau$ . The frequency spacing between two adjacent sub-carriers in truncated OFDM signals is defined as  $\frac{1}{T_{OFDM}}$  which is the same as that of OFDM signals. The equation of the transmitted signal is thus given as:

$$x(t) = \frac{1}{\sqrt{T_{OFDM}}} \sum_{l=-\infty}^{\infty} \sum_{n=0}^{N-1} F_{l,n} \exp\left(\frac{j2\pi(t - l\tau T_{OFDM})}{T_{OFDM}}\right) \quad (1)$$

where  $F_{l,n}$  is the data symbol modulated on the  $n^{th}$  sub-carrier and  $l^{th}$  OFDM symbol,  $N$  represents the index of the sub-carrier and  $\frac{1}{\sqrt{T_{OFDM}}}$  is a normalization factor. The truncated OFDM symbol can be given as a function of the transmitted OFDM symbol i.e.  $T_{OFDM} = \tau T_{OFDM}$ . With this, equation 1 can be re-written as:

$$x(t) = \frac{1}{\sqrt{T_{OFDM}}} \sum_{l=-\infty}^{\infty} \sum_{n=0}^{N-1} F_{l,n} \exp\left(\frac{j2\pi(t - lT_{OFDM})}{T_{OFDM}}\right) \quad (2)$$

Due to the time truncation factor  $\tau$ , the transmitted subsequent symbol arrives earlier in time by  $(1 - \tau)$  due to the truncation of the preceding symbol. The generated truncated OFDM signals are not orthogonal when compared with their OFDM



counterpart in higher transmission rates of each sub-carrier since the truncated OFDM symbol duration is not equal to the reciprocal of the frequency spacing between the sub-carriers e.g. ten truncated OFDM symbols may be sent in the same time slot as eight OFDM ones.

By sampling one truncated OFDM symbol with sample period  $T_{OFDM}/H$ , where  $H = \rho N$  and  $\rho \geq 1$  is the oversampling rate, the process of modulating the input data onto different sub-carriers in a discrete truncated OFDM symbol is expressed as [10]:

$$X(k) = x\left(\frac{kT_{OFDM}}{H}\right) = \frac{1}{\sqrt{\tau H}} \sum_{n=0}^{H-1} F_n \exp\left(\frac{j2\pi nk}{H}\right) \quad (3)$$

where  $k$  is the index of the time sample of the truncated OFDM symbol for the range  $0 \leq k \leq \tau H - 1$ . Equation 3 can be written in matrix form as [10]:

$$X = \Phi * F \quad (4)$$

$X = [x_0, x_1, \dots, x_{\tau H-1}]^T$  denotes a  $\tau H$ -dimensional vector that is a sampled truncated OFDM symbol in the time domain,  $F = [f_0, f_1, \dots, f_{\tau H-1}]^T$  is an  $N$ -dimensional vector that is a sampled input data in the frequency domain.  $\Phi$  denotes a two-dimensional sampled carrier matrix i.e.  $\tau H \times H$ . The elements of sub-carrier matrix  $\Phi$  are given by  $\Phi_{k,n} = \frac{1}{\sqrt{\tau H}} \exp(j2\pi nk/H)$ , where  $0 \leq k \leq H - 1$  and  $0 \leq n \leq \tau H - 1$ .

#### A. Sample Mapper for FMRM Scheme

Table I shows a typical mapping strategy for FMRM that conveys three bits per timeslot, thereby activating various ranks depending on the transmitted bit. The pattern of the  $n_s$  subcarriers is given by the positions,  $\mathbf{p}$  where the subcarrier is used in the OFDM transmission. A simple case where known signals are transmitted is presented in this paper.

Table I: Mapping Table for FMRM

Input Bits	Frequency Index (MHz)	Rank
000	$f_1$	1
001	$f_1, f_2$	2
010	$f_1, f_2, f_3$	3
011	$f_1, f_2, f_3, f_4$	4
100	$f_1, f_2, f_3, f_4, f_5$	5
101	$f_1, f_2, f_3, f_4, f_5, f_6$	6
110	$f_1, f_2, f_3, f_4, f_5, f_6, f_7$	7
111	$f_1, f_2, f_3, f_4, f_5, f_6, f_7, f_8$	8

#### B. Signal Transmission

In the transmission presented in this paper, a modulated signal  $x(t)$  experiences an Additive White Gaussian (AWGN) noise  $n = [n_1 n_2 \dots n_{N_r}]^T$ , where  $N_r$  denotes the number of receive antennas. The received signal is given by

$$\mathbf{y}(t) = \sqrt{\bar{\gamma}} \mathbf{x} + \mathbf{n} \quad (5)$$

where  $\bar{\gamma}$  is the average signal to noise ratio (SNR) at each of the receive antennas. The noise,  $n$  has the distribution  $\mathcal{CN}(0, 1)$  with independent and identical (i.i.d.) entries.

Breaking down the signal component  $\mathbf{x}$  of (5) gives the sinusoid,

$$\mathbf{x} = \sin \omega t \quad (6)$$

$\omega$  can further be broken down to its simpler form i.e.

$$\omega_i = 2\pi f_i \quad (7)$$

Thus, we have

$$\mathbf{y} = \sqrt{\bar{\gamma}} \left( \sum_i \sin 2\pi f_i t \right) + \mathbf{n} \quad (8)$$

This paper focuses on the frequency component of the modulated signal as given in (8) by varying the frequency  $f_i$  during transmission. This has an effect of activating a different rank during the transmit activity where each rank contains a given number of transmit frequencies with the minimum being one. At the receiver, the frequency MRM detector estimates the rank of the transmitted signal, which is then used to decode the transmitted input bits in the frequency domain.

#### C. Signal Detection for Maximum Likelihood (ML)

At the receiver, the received signals are detected by Fast Fourier Transform (FFT) and demodulated in order to decode the conveyed bits. Due to the nature of the transmitted symbols being equally likely at the receiver, an optimal FMRM detector is used to perform detection of the known modulation symbol.

FFT operation is performed on the received signals to form frequency signals,  $Y$ , and the threshold detector is applied on the absolute amplitude of the frequency signal. The amplitude at each subcarrier is expressed in the following vector,  $\mathbf{v}$ , i.e.

$$\mathbf{v} = (2 \cdot |Y(f_i)|), \quad i \in [1 : n_s] \quad (9)$$

where  $n_s$  is the total number of subcarriers given in the mapping table.

A threshold detector is then used to check if the amplitude at subcarrier,  $i$  is greater than a threshold value,  $\delta$ , for formation of the output subcarrier positions  $\hat{\mathbf{p}}$ .

$$\hat{\mathbf{p}} = \min(|\mathbf{v}(i) - \delta| > 0) \quad (10)$$

The output pattern formed from these subcarrier positions is used to demap the conveyed information according to table one.

#### D. Signal Detection for Selection Combining (SC)

When multiple receive antennas are deployed at the receiver, then the simple SC technique can be used to enhance reliability of the received signals. Under SC, the combiner selects the receive branch with the highest signal power, such that

$$\mathbf{v} = \max_j (2 \cdot |Y(f_i, j)|), \quad i \in [1 : n_s] \quad j \in [1 : N_r] \quad (11)$$

### III. SYSTEM PERFORMANCE ANALYSIS

In this section, the system performance is analyzed under AWGN signals. For Bit Error Probability (BEP) analysis, we use Binary Phase Shift Keying (BPSK) modulation where the binary symbols last for  $T_s$  seconds each during transmission, and are characterized by the phase of the carrier i.e.

$$s_i(t) = A \cos(2\pi f_c t + \phi_i) \quad (12)$$

where  $0 \leq t \leq T_s$  for  $i = 1, 2$  and  $f_c$  is the carrier frequency. The transmit antenna will transmit  $s_1(t)$  when the bit is zero and  $s_2(t)$  when the bit is one. The maximum possible phase difference between the two bits is  $\pi$ . Assuming  $\phi_1 = 0$  and  $\phi_2 = \pi$ , the two signals will thus be:

$$\begin{aligned} s_1(t) &= A \cos(2\pi f_c t), 0 \leq t \leq T_s \\ s_2(t) &= \cos(2\pi f_c t + \pi) \\ s_2(t) &= -A \cos(2\pi f_c t), 0 \leq t \leq T_s \end{aligned} \quad (13)$$

#### A. Bit Error Probability

Taking into account an AWGN channel where  $h = 1$ , the received signal in equation (5) can thus be modeled as:

$$y = x + n \quad (14)$$

where  $n \sim \mathcal{CN}(0, \sigma^2)$ ;  $\sigma^2 = N_o$ ;  $x \in (-A, A)$  and  $SNR = \hat{\gamma} = \frac{A^2}{\sigma^2}$ . Re-writing equation (14) with  $n$  as the subject gives:  $n = (y - x)$ ,  $\bar{n} = (y + \sqrt{A})$ .

The probability density function,  $P$  can thus be expressed as:

$$P = \frac{1}{\sqrt{2\pi\sigma^2}} \int_0^\infty \exp\left(\frac{-n^2}{2\sigma^2}\right) dn \quad (15)$$

For BPSK, only the real part of the signal is considered, where  $N_o = \frac{\sigma^2}{2}$ . Therefore, the BER for BPSK is given as,

$$P_e = Q\left(\sqrt{\frac{2A}{\sigma^2}}\right) = Q\left(\sqrt{2\hat{\gamma}}\right) \quad (16)$$

where  $\hat{\gamma} = \psi_o \bar{\gamma}$ , is the effective SNR that consists of oversampling gain,  $\psi_o$  and  $A = \delta$  and  $Q(x) = \frac{1}{\pi} \int_0^{\frac{\pi}{2}} \exp\left(\frac{-x^2}{2 \sin^2 \theta}\right) d\theta$ . Applying trapezoidal rule to (16) yields,

$$Q(x) = \frac{1}{2t} \left( \frac{1}{2} \exp\left(\frac{-x^2}{2}\right) + \sum_{k=1}^{t-1} \exp\left(\frac{-x^2}{S_T}\right) \right) \quad (17)$$

where  $S_T = 2 \sin^2\left(\frac{T\pi}{2t}\right)$  and  $t$  is the number of iterations used in the approximation. The bit error probability is written as,

$$BEP_{AWGN} = \frac{1}{2t} \left( \frac{1}{2} \exp(-\hat{\gamma}) + \sum_{k=1}^{t-1} \exp\left(\frac{-2\hat{\gamma}}{S_T}\right) \right) \quad (18)$$

Under diversity reception, the BER is given as,

$$BEP_{AWGN}^d = (BEP_{AWGN})^{N_r} \quad (19)$$

### IV. SIMULATION RESULTS AND DISCUSSIONS

Here, analytical results derived in the previous sections are validated via Monte Carlo simulations. We demonstrate the system's performance by comparing the simulation results and analytical results for one bit, two bits and three bits transmission, respectively. Fig. 2 shows that the analytical expression for BER closely follows the simulation results for all the three cases of 1-bit, 2-bits, and 3-bits transmission. Two subcarriers are used in the case of 1-bit, Four subcarriers for the 2-bits and Eight subcarriers for the case of 3-bits transmission. Therefore, the gain coefficient of oversampling are given by  $\psi_o = 8, 2, 0.25$ , respectively.

Fig. 3 depicts the comparison of FMRM with MQAM schemes at the same data rates. It is evident that the oversampling and detection method employed for FMRM is superior to those employed for conventional MQAM modulation. 1-bit MRM requires less power than BPSK of about 8[dB]. Similarly, 2-bits MRM requires less power than 4QAM of about 8[dB]. However, since  $\psi_o = 0.25$  in the case of 3-bits transmission, FMRM is just about better than 8QAM. This means that the detector employed for FMRM plays a significant role in producing lower error rates. For these cases, the threshold for detection was set at  $\delta = 0.6$ .

Fig. 4 shows BER results for different receive antennas, which are exploited in the case of receive diversity. Here, SC combiner is used to select the branch with the highest signal power. It is shown that FMRM system is consistent with such SC configuration and the BER decreases with increases in the number of receive branches. Furthermore, the simulation results closely match the theoretical results as presented in this paper.

The detector employed in this paper depends on the threshold value  $\delta$ . It is therefore important to present results due to variation of  $\delta$ . Fig. 5 shows the results when  $\delta$  is varied in the range  $\delta = [0.6 \ 0.65 \ 0.7]$  for the case of 2-bits transmission. It can be observed that the desired detection threshold to be 0.6 as it is the one that is validated by the theoretical framework and yields expected results. The detection threshold can be increased only if the transmission power is also increased, but since the aim of a system is to save on power as well, the 0.6 threshold is the desirable threshold for the system under an AWGN channel.

### V. CONCLUSION

An FMRM communication system has been presented that provides flexible data rates for index modulation systems. Moreover, it has been demonstrated that both simulation results and the proposed analytical framework results agree. The FMRM system may therefore be adopted to mitigate the limitations in conventional MRM, especially in changing data rates. It has been further demonstrated that FMRM introduces flexibility in increasing reliability over conventional BPSK, and MQAM at equal data rates and has security advantages introduced by the addition of the information mapper. Further work can be conducted for the same system over flat-fading Rayleigh and Rician Channels.

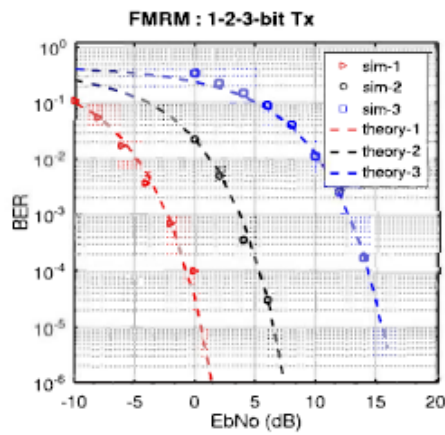


Fig. 2. BER comparison at different data rates, (1, 2, 3) bits

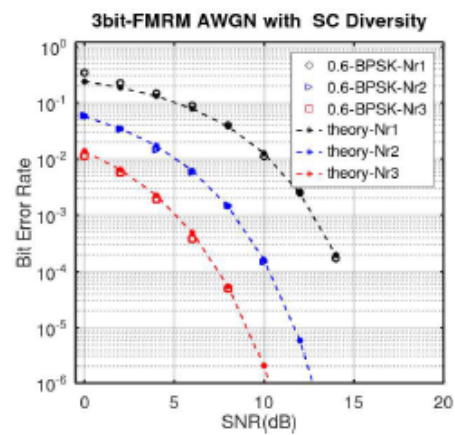


Fig. 4. BER for 3Bits Tx FMRM with SC Diversity in AWGN channel

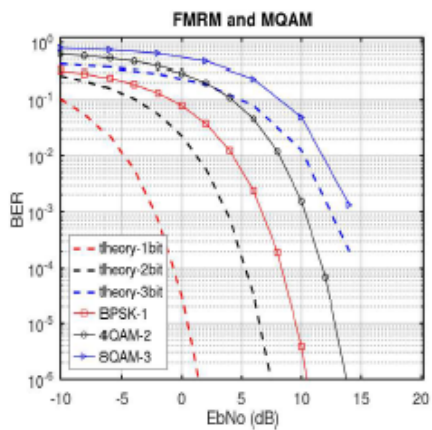


Fig. 3. BER comparison of FMRM with MQAM, (1, 2, 3) bits

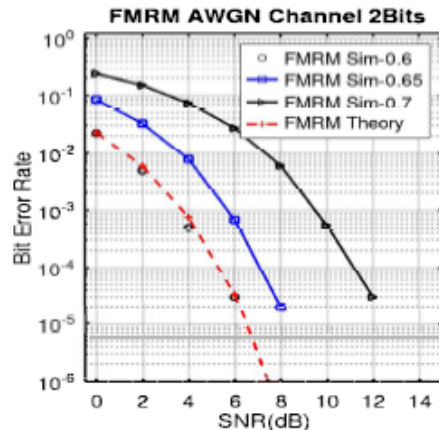


Fig. 5. BER for 2Bits Tx FMRM with varying threshold detection in AWGN channel

## REFERENCES

- [1] Wang, Q., Chang, Y., Yang, D.: 'Deliberately designed asynchronous transmission scheme for MIMO systems,' IEEE Signal Processing Letters, 14, pp. 920-923, 2007.
- [2] R. Mesleh, H. Haas, C. Ahn, and S. Yun, "Spatial modulation- a new low complexity spectral efficiency enhancing technique," First international Conference on Communications and Networking in China (ChinaCom'06), pp.1-5, Oct. 2006.
- [3] E. Basar, "Index modulation techniques for 5G wireless networks," IEEE Commun. Mag., vol. 54, no. 7, pp. 168-175, June 2016.
- [4] H. Haas and M. Di Renzo, "Enhanced spatial modulation," U.S. Patent 20130058390, Feb. 23, 2010.
- [5] P. Akuon and H. Xu, "Polar coded spatial modulation," IET Commun., vol.8, no. 9, pp. 1459 - 1466, 2014.
- [6] E. Basar, U. Aygolu, E. Panayirci, and H. V. Poor, "Orthogonal frequency division multiplexing with index modulation," IEEE Trans. Signal Process., vol. 61, no. 22, pp. 5536-5549, Nov. 2013.
- [7] P. Akuon and H. Xu, "A multiple Rank Modulation System," SA 2015, US Patent 2018/0269944 A1, 2018.
- [8] A. Nyawade, P. Akuon and H. Xu, "Spatial MIMO Rank Modulation," IEEE Africon, Accra, Ghana, 2019.
- [9] P. Akuon and A. Mwangi, "Systems and Methods for Communication," Patent Application, PCT/IB2017/056785, 2018.
- [10] S. Isam and I. Darwazeh, "Characterizing the intercarrier interference of non-orthogonal Spectrally Efficient FDM system," Communication Systems, Networks and Digital Signal Processing (CSNDSP), 2012 8th International Symposium on, Poznan, 2012, pp. 1-5.

# Frequency MIMO Rank Modulation

Nyanjom Jack Onyango and Peter O. Akuon

School of Engineering, University of Nairobi  
Nairobi, Kenya

[jack.nyanjom@gmail.com](mailto:jack.nyanjom@gmail.com), [akuon@uonbi.ac.ke](mailto:akuon@uonbi.ac.ke), [akuonp@yahoo.com](mailto:akuonp@yahoo.com)

**Abstract** - A transmission technique, referred to as frequency multiple-input multiple-output (MIMO) rank modulation (FMRM), is proposed that uses multiple frequency domains (i.e. ranking domains) only to convey information to the receiver. In FMRM, the number of active transmit antennas or the rank of each frequency domain is determined by the structure of the information input bits. The input information bitstream, which is random, is sent into the ranking modulator. Instead of detecting the channel index, the receiver detects the number of paths of the received radio frequency (RF) signals. In FMRM, the transmitted signals are pre-set and known at the receiver using the system mapper. Only the rank information is used to decode the bits in the ranking domain. Analytical upper bounds on bit error probability (BEP) of the FMRM system will be derived based on principal component analysis (PCA) of the sample covariance of the signals in the detector. Analytical results will then be compared with simulation results at different data rates which show tractable performance. For better information security operations, the FMRM system has the additional benefit that the wireless channel does not completely modulate the information sent, but the information is also modulated by the number of RF chains.

**Index Terms** — MIMO, rank modulation; multiple frequency domains; modulation domain; radio frequency (RF) chains

## I. INTRODUCTION

The basis for the MIMO concept is to increase data rates and reliability by exploiting simultaneous transmission of different signals. High spectral efficiency and reliability can be achieved through spatial multiplexing or spatial diversity like vertical Bell Labs Layered Space-Time (VBLAST) architecture [1]. However, these schemes suffer from high inter-channel interference (ICI) and they require inter-antenna synchronization (IAS) to avoid inter-symbol interference (ISI). Also, the detection algorithms at the receiver for MIMO systems have high complexity and the number of receive antennas is required to be equal to or more than the number of transmit antennas. Therefore, as usual, some trade-offs are required so that practical MIMO schemes are achieved. To date, several alternative MIMO schemes have been proposed. Antenna selection schemes, asynchronous transmission and spatial modulation (SM) present admirable trade-offs for conventional MIMO schemes [2-3].

SM is an inventive technique that conveys some information to the receiver based on the spatial signature of the received signal. The spatial signature in SM is provided by the transmit antenna and when the transmit antenna is detected at the receiver then

the spatial information is decoded. This is possible because it is the spatial information that selects the active transmit antenna. In the conventional SM, only one modulation symbol is transmitted to the receiver by one active transmit antenna per symbol period. Then, both the modulation symbol and the transmit antenna are jointly detected at the receiver. Therefore, ICI is avoided completely, and data rates are still enhanced through spatial information. Furthermore, spatial information alone can be utilized to transmit information to the receiver. Such a system has been presented as space-shift keying modulation (SSK) in [4].

However, the following concerns can be assessed further in SM systems. The spectral efficiency (SE) of SM increases logarithmically with the number of transmit antennas ( $N_t$ ) i.e.  $SE = \log_2(MN_t)$ , where  $M$  denotes the modulation index. Therefore, the data rates in SM are lower than VBLAST. Also, the number of transmit antennas is required to be a power of two. This requirement needs a large number of antennas. However, fractional bit encoded (FB-SM), generalized spatial modulation (GSM) and generalized space shift keying (GSSK) can be used to reduce the number of transmit antennas [5-6]. Furthermore, the wireless channel is the spatial modulator in SM and the detection process may lead to error in the spatial domain in the case where the channels are similar. To this end, power detection has been proposed in the patent by Harald Haas and Marco Di Renzo in enhanced spatial modulation (ESM) [7]. In ESM, the transmit element is detected using the knowledge of the power allocated at the transmitter to decode the spatial bits i.e. the location of the active transmitter element is detected using the knowledge of the power allocated to the transmitter elements [8]. Similarly, in polar coded spatial modulation (PCSM), the channel rate or the number of bits in the frozen set can be used to relay spatial information to the receiver without encountering any channel errors [8].

In the proposed MRM scheme, when the frequency domain is configured to convey information, then a secure system is devised. Therefore, the detection errors for modulation information in MRM arise from the conventional amplitude and phase modulation (APM) schemes and the multiplicity of the ranking domain. Mainly, MRM exploits different transmit MIMO RF chains to convey information to the receiver.

## II. RESEARCH PROBLEM

With the growing demand for higher data rates, MIMO systems have become the main focus for communication systems.

Peter O. Akuon, PhD, is a lecturer in the Department of Electrical & Information Engineering at the University of Nairobi (e-mail: [akuon@uonbi.ac.ke](mailto:akuon@uonbi.ac.ke)).

Nyanjom Jack Onyango is undertaking Master of Science in Electrical & Electronics Engineering at University of Nairobi, Kenya (e-mail: [jack.nyanjom@gmail.com](mailto:jack.nyanjom@gmail.com)).  
UNIVERSITY OF NAIROBI

Spatial modulation (SM) being a recent technology has several advantages over other MIMO schemes. In addition to the modulation signal, SM utilizes antenna index as a source of information to increase transmission capacity, avoid some level of synchronization and Inter-Channel Interference (ICI).

However, the utilization of an index for the transmission antenna as a source of data implies that if the channels look alike, then spatial information may be lost completely. This is because just like all the variants of SM technology like Space Shift Keying (SSK), Double Spatial Modulation (DSM), and Generalized Space Shift Keying (GSSK), the SM detector uses the shape of each channel to detect spatial information. There may be cases in the user market that may lead to the reception of signals that look alike due to the similarity of channels e.g. in signal correlation [9].

In Enhanced Spatial Modulation (ESM), the received signal power can be used to detect the spatial information where each activated transmit antenna transmits at a known power level. However, this leads to other implementation implications at the transmission system and feedback may be required from the recipient system. Also, in Polar Coded Spatial Modulation (PCSM), different rates can be used to transmit known frozen bits and then use the rate or capacity information to decode the spatial bits with minimal error or in the control channel.

However, coset-coding is required to achieve this technique [9]. Therefore, there is the need for an enhanced Spatial Modulation technique as well as transmitting and receiving devices through the use of MRM for decreasing the high demodulation complexity and errors in the spatial domain, while providing additional capacity and data rates.

### III. METHODOLOGY

OFDM is used to improve on SM by leveraging the use of frequency to enhance Multiple Rank Modulation. The received signal model is given by:

$$y = h * x + n \quad (1)$$

where  $h$  is the channel impulse response,  $x$  is the modulated symbol using OFDM and  $n$  is additive white gaussian noise. Breaking down the modulated symbol component of equation (1) gives the equation of a sinusoid i.e.:

$$x = \sin wt \quad (2)$$

$w$  can further be broken down to its simpler form i.e.

$$w = 2\pi ft \quad (3)$$

The overall equation (1) thus becomes:

$$y = h * 2\pi ft + n \quad (4)$$

The paper focuses mainly on the frequency component as illustrated in equation 4 by varying it during transmission. This has an effect of activating a different rank during the transmit

activity where each rank contains a given number of antennas with the minimum being one.

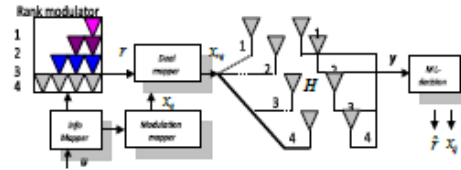


Figure 1-System Model: MIMO Rank Modulation

TABLE I  
MAPPING TABLE FOR FREQUENCY MRM

Input Bits	Frequency Index	Rank
000	$f_1$	1
001	$f_1, f_2$	2
010	$f_1, f_2, f_3$	3
011	$f_1, f_2, f_3, f_4$	4
100	$f_1, f_2, f_3, f_4, f_5$	5
101	$f_1, f_2, f_3, f_4, f_5, f_6$	6
110	$f_1, f_2, f_3, f_4, f_5, f_6, f_7$	7
111	$f_1, f_2, f_3, f_4, f_5, f_6, f_7, f_8$	8

MATLAB codes have been used to develop a simulation model for Frequency coded Multiple Rank Modulation. The BER criteria are used to test the system performance where the error rates are plotted against various SNR ranges. The Capacity of the channel is also tested using the various coding mechanisms. Multiple receive antennas are tested under the simulation model. In the simulation model, the three parameters that are varied interchangeably are Power levels of SNR, Number of Antennas and Multiplicity of the Frequency. A validation formula that predicts the performance of the simulations through a mathematical approach is also established.

Different symbols can be used in modulation i.e. MQAM, PSK, BPSK, APSK, PCM, AM, FM, OFDM. For this paper, Orthogonal Frequency Division Multiplexing is used to perform the tests. Channel modelling is dependent on the degree of existence of a line of sight between the receive and transmit antennas [2].

### IV. RESULTS

BER to SNR (Eb/No) [dB] curves yield results as shown below i.e. the theoretical framework validation curves vis a vis the simulated curves match or slightly differ for identical parameters e.g. the same number of transmit antennas and receive antennas. The system performance increases with an increase in the number of antennas e.g. if one transmitting antenna is used, at the receiver side as the number of receive antennas increase, the system performance increases and the curves tend towards zero (0). If two transmitting antennas are used and the number of receive antennas is varied, the system

performance improves further and becomes better than the first scenario explained.

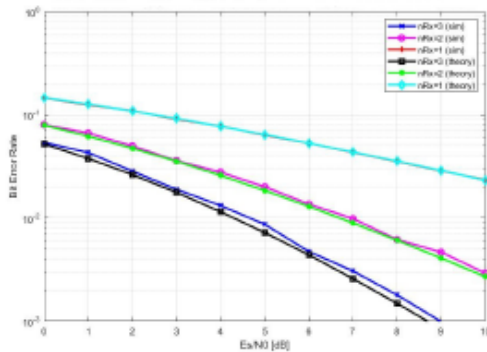


Figure 2-Using Selection Combining (SC) at the receiver

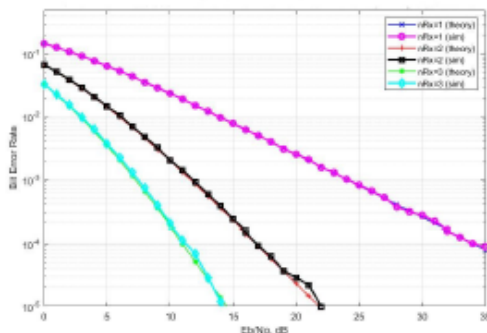


Figure 3-Using Equal Gain Combining (EGC) at the receiver

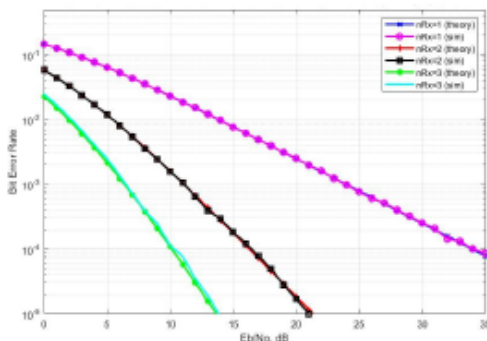


Figure 4-Using Maximal Ratio Combining (MRC) at the receiver

## V. CONCLUSION

Frequency MRM is useful in increasing information security where various antenna nodes are used to convey information. The receiver would have to know the number of antennas or the mapping table. Besides, the transmitted information can be conveyed without exploiting the conventional symbol modulation space. Nevertheless, just like conventional MIMO system, there are physical limitations of MRM in terms of

UNIVERSITY OF NAIROBI

implementation of RF chains. This is because each antenna head may require an independent RF structure. Further tests will be performed to study cases where MRM conveys the transmitted information under correlated channels.

## REFERENCES

- [1] R. A. Horn and C. R. Johnson, *Matrix Analysis*. Cambridge, UK: Cambridge University Press, 1990.
- [2] Wang, Q., Chang, Y., Yang, D.: 'Deliberately designed asynchronous transmission scheme for MIMO systems,' *IEEE Signal Processing Letters*, 14, pp. 920-923, 2007
- [3] R. Mesleh, H. Haas, C. Ahn, and S. Yun, "Spatial modulation- a new low complexity spectral efficiency enhancing technique," First international Conference on Communications and Networking in China (ChinaCom'06), pp.1-5, Oct. 2006.
- [4] M. Di Renzo and H. Haas, "Space shift keying (SSK) modulation with partial channel state information: Optimal detector and performance analysis over fading channels," *IEEE Trans. on Commun.*, vol. 58, no.11, pp. 3196-3210, 2010.
- [5] N. Serafimovski, M. D. Renzo, S. Sinanovic, R. Y. Mesleh, and H. Haas, "Fractional Bit Encoded Spatial Modulation (FBE-SM)," *IEEE Commun. Lett.*, vol. 14, no. 5, pp. 429-431, May 2010.
- [6] J. Jeganathan, A. Ghayeb, L. Szczecinski, "Generalized space shift keying modulation for MIMO channels," in Proc. IEEE 19<sup>th</sup> International Symposium on Personal, Indoor and Mobile Radio Communications PIMRC 2008, Cannes, France, 15-18 September 2008
- [7] H. Haas and M. Di Renzo, "Enhanced spatial modulation," U.S. Patent 20130058390, Feb. 23, 2010
- [8] P. Akuon and H. Xu, "Polar coded spatial modulation," *IET Commun.*, vol.8, no. 9, pp. 1459 - 1466, 2014.
- [9] H.Xu, P.Akuon. 2017. A Multiple Rank Modulation System. WO2017037562



# Receive Diversity on Correlated Rayleigh Fading Channels based on IEEE 802.11n Wi-Fi Standard

Jack O. Nyanjom and Dr. Peter O. Akuon  
School of Engineering, University of Nairobi  
Nairobi, Kenya

[jack.nyanjom@gmail.com](mailto:jack.nyanjom@gmail.com), [akuon@uonbi.ac.ke](mailto:akuon@uonbi.ac.ke), [akuonp@yahoo.com](mailto:akuonp@yahoo.com)

**Abstract**— An error analysis method of Maximal Ratio Combining (MRC) in Rayleigh fading channel is presented based on Wi-Fi technology. With the need for faster data rates, lower latency and improved reliability, there is need to find an optimal scheme that can achieve this. This paper aims to address how to improve on these using receive diversity. With the implementation of 5G, it will be possible to provide very fast speeds but more importantly it will have enough capacity to perform every function intended without drop in speed or connectivity regardless of the number of people simultaneously connected. It will run on new high-spectrum bands which uses higher frequency signals than the current 4G thus making them much less congested currently. IEEE 802.11n supports any number of antennas between one and four and thus it is possible that one device may have three antennas while another with which it is communicating will only have two. The supposedly surplus antenna can be used to provide diversity reception. Error performance of MRC being better, it is used to analyze the reception diversity by varying the number of antennas at the receiver. Extensive simulations for average bit error probability, which show tight bounds with the proposed analytical approach are undertaken. Channel correlations for different practical antenna spacing of 0.1, 0.2 and 0.5 of the signal carrier wavelengths are analyzed.

## I. INTRODUCTION

Diversity techniques are among the prominent ways to improve the reliability of wireless communication systems [1, 2]. The main idea of diversity is to extract information from the received signal components transmitted over multiple fading channels to improve the received signal-to-noise ratio (SNR) [3, 4]. Receive diversity combining techniques are usually utilized in applications that employ multiple antenna elements in order to improve the figures of merit of the combined signal. In wireless communications, received signals can be combined through three principal techniques namely, maximal ratio combining (MRC), selection combining (SC) and equal gain combining (EGC) [5]. The choice of any of these techniques depends on the tradeoff between complexity costs and reliability.

Generally, EGC and SC have lower complexity costs than the MRC yet, this comes at the expense of high

signal errors, which is the tradeoff figure of merit. The close-enough spacing is essential in order to make sure that the received signals are correlated, which is an essential requirement to acquire the full benefit of the diversity receiver [6]. The performance of diversity methods has been extensively examined in the literature for Rayleigh fading. If the channel is perfectly estimated at the receiver, MRC can be applied to maximize the output SNR and minimize the bit error rate (BER) [7].

However, due to the fact that channel estimation is often imperfect in practice, the estimation error will decay the system performance. This has been investigated in [8, 9], but the recent evolutions in mobile communication systems have renewed the attention in comprehending and mitigating the effect of imperfect channel estimation on diversity techniques [10]. The error performance of MRC in Rayleigh fading environment with independent and identically distributed (i.i.d.) diversity branches is investigated in [11]. In [12], the SNR distribution is given for similar scenarios. In [13], the error performance of MRC with independent but not identically distributed (i.n.d.) branches is studied.

An error analysis method of MRC in Rayleigh fading channel is presented based on Wi-Fi technology.

## II. SYSTEM MODEL

In this paper, it is assumed that the information bits are modulated by binary phase-shift keying (BPSK) modulation. The channel is assumed to be frequency nonselective and slowly fading over the length of the transmitted symbol. We also assume that  $M$  diversity branches are employed at the receiver for reception. In addition, this paper assumes the diversity branches are sufficiently close to each other, so that the received signals are correlated. The received signal model under correlation is given by:

$$y = \hat{h} * x + n \quad (1)$$

where:  $\hat{h} = A * h$ ,  $h$  is channel impulse response,  $x$  is modulated symbol - BPSK,  $n$  is additive white gaussian noise and  $A = Q * \sqrt{D}$ .

The values  $Q$  and  $D$  are obtained from the Singular Value Decomposition (SVD) of the normalized correlation matrix  $R$  (the factorization of  $R$  into a product of three matrices) where  $Q$  is the position matrix of eigenvectors whose columns are orthonormal and  $D$  is the diagonal matrix whose elements are Eigen-values with positive real entries. The correlation matrix  $R$  considers the Wi-Fi standard adopted in terms of both frequency and spacing among antennas at the Wi-Fi device.

### 2.1 Channel Correlation

We model system correlation among the antennas using the conventional method. The correlation coefficient  $\rho_{kl}$  between the  $k$ th and the  $l$ th branch is given as [5, eqn. (45)]

$$\rho_{kl} = \frac{E[\hat{h}_k \hat{h}_l]}{\sqrt{\sigma^2_{\hat{h}_k} \sigma^2_{\hat{h}_l}}}, \quad 1, k=1, 2, \dots, N_r \quad (2)$$

where  $\sigma^2_{\hat{h}_k}$  and  $\sigma^2_{\hat{h}_l}$  denote the variance of the random variables  $\hat{h}_k$  and  $\hat{h}_l$  respectively. The normalized correlation matrix  $R$  is thus given by [5]

$$R = \begin{bmatrix} 1 & \rho_{12} & \dots & \rho_{1N_r} \\ \rho_{21} & 1 & \dots & \rho_{2N_r} \\ \vdots & \vdots & 1 & \vdots \\ \rho_{Nr1} & \dots & \dots & 1 \end{bmatrix} \quad (3)$$

It is assumed that the formed correlation matrix from (3) is positive definite so that so that it has positive eigenvalues [14].

### 2.2 Diversity Combining and Equalization

In diversity systems, the received signals are equalized through a filter  $\omega_c$  in order to obtain the symbol estimate  $\hat{x}_{0,c}$ . The equalised symbol is written as [5]

$$\hat{x}_{0,c} = w_c^H \hat{s} = w_c^H \hat{h} x + w_c^H n \quad (4)$$

where  $c$  denotes the type of the combiner, i.e. EGC, SC, MRC. In the case of MRC  $w_c = \hat{h}$ .

## III. MRC SCHEME

In MRC, the receiver linearly combines the received signal  $y_i(t)$  with  $\omega_i$ , which is the weighting coefficient of the  $i$ th branch. The output signal  $y(t)$  of the linear diversity combiner is then given by

$$y(t) = \sum_{i=1}^M w_i y_i(t) = S(t) \sum_{i=1}^M w_i g_i + \sum_{i=1}^M w_i n_i \quad (5)$$

where  $g_i$  is the channel gain at two different diversity branches and is assumed to be identically distributed,  $n_i$  is the random noise variable which is complex additive white gaussian noise (AWGN). Since  $S(t)$  is assumed to have unit power, SNR at the output of combiners is

$$\gamma_T(\hat{w}) = \frac{1}{\sigma_n^2} \frac{|\sum_{i=1}^M w_i g_i|^2}{\sum_{i=1}^M |w_i|^2} = \frac{|\hat{w} \hat{G}^T|^2}{E\{|\hat{w} \hat{N}^T|^2\}} \quad (6)$$

$$E\{|\hat{w} \hat{N}^T|^2\} = E\{|\hat{w} \hat{N}^T \hat{w}^T \hat{N}|\} = \sigma_n^2 \hat{w}^2 \quad (7)$$

According to the Cauchy-Schwarz inequality, MRC with perfect channel estimation has maximum output SNR among all methods if  $\hat{w}$  is linearly proportional to  $\hat{G}$ . If  $\hat{w} = \hat{G}$  this implies that  $\gamma_T = |\hat{G} \hat{G}^T|^2 / \sigma_n^2 \hat{G}^T \hat{G} = \hat{G} \hat{G}^T / \sigma_n^2 \Rightarrow \gamma_T = \sum_{i=1}^M |\gamma_i|$ , the output SNR is thus the sum of the SNR at each element. Using the above assumption, the expected value of the output SNR is therefore  $M$  times the SNR at each branch. For imperfect channel estimation, which is the main issue in practice, it is observable that the SNR is highly dependent on  $\omega_i$ .

The optimal solution is the weighting vector, which maximizes the objective function  $\gamma_T$  in (6). We assume  $p_i$  is the estimate of the complex gain  $g_i$  on the  $i$ th diversity branch and  $e_i$  is the estimation error with zero mean and variance  $\sigma_e^2 = \sigma_g^2 (1 - \rho^2)$  where  $\rho \in [0, 1]$  is the normalized estimation error correlation coefficient.

Under Gaussian error model,  $g_i$  and  $p_i$  are related as  $g_i = p_i + e_i$  [15]. According to the diversity combining rule, the combiner's weights take on the  $\omega_i = p_i^*$  for MRC diversity, which is based on the Cauchy-Schwarz inequality, maximizes (6) if the channel is perfectly estimated (i.e.,  $\rho=1$ ). However, since channel estimation is often imperfect in practice, the MRC is a suboptimal solution [16-36].

## IV. SIMULATION AND RESULTS

We have used IEEE 802.11n standard taking 5GHz as the frequency of choice which lies in between the first range of 5G frequencies i.e. 600MHz to 6GHz. Diversity uses the multiple antennas available and combines or



selects the best subset from a larger number of antennas to obtain the optimum signal conditions. This can be achieved because there are often surplus antennas in a MIMO system. 802.11n supports any number of antennas between one and four and thus it is possible that one device may have three antennas while another with which it is communicating will only have two. The supposedly surplus antenna can be used to provide diversity reception or transmission as appropriate.

To obtain the value of lambda we use the formula:

$$\lambda = \frac{c}{f} \quad (8)$$

where c is the speed of light. Taking  $f = 5\text{GHz}$  and  $c = 2.99792458 \times 10^8 \text{m/s}$ ,

$$\lambda = \frac{2.99792458 \times 10^8}{5.0 \times 10^9} = 0.059958\text{m} \approx 0.06\text{m}$$

The signals received by the antennas will be correlated depending on the size of the antenna spacing. An assumption is made in the correlation model in that the linear array of antennas has a uniform angle of arrival distribution. The correlation coefficient,  $\rho$  can be obtained from the formula:

$$\rho = J_0\left(2\pi\frac{d}{\lambda}\right) \quad (9)$$

where  $J_0(\cdot)$  denotes the zero-order Bessel function of the first kind, d denoted the spacing between antennas and  $\lambda$  denotes the wavelength of the carrier. Taking the values of  $d = 0.5\text{cm}, 0.2\text{cm}, 0.1\text{cm}$  and  $\lambda = 0.06\text{m}$ , the correlation coefficient gives:

$$\rho = J_0\left(2\pi\frac{0.005}{0.06}\right) = J_0\left(\frac{1}{6}\pi\right) \quad (10)$$

$$\rho = J_0\left(2\pi\frac{0.002}{0.06}\right) = J_0\left(\frac{1}{15}\pi\right) \quad (11)$$

$$\rho = J_0\left(2\pi\frac{0.001}{0.06}\right) = J_0\left(\frac{1}{30}\pi\right) \quad (12)$$

From the values of  $\rho$  above, we can compute the values of the normalized correlation matrix, R, with  $d = 0.5\text{cm}, 0.2\text{cm}$  and  $0.1\text{cm}$  respectively.

$$R = \begin{bmatrix} 1 & 0.9326 & 0.7441 & 0.4720 \\ 0.9326 & 1 & 0.9326 & 0.7441 \\ 0.7441 & 0.9326 & 1 & 0.9326 \\ 0.4720 & 0.7441 & 0.9326 & 1 \end{bmatrix} \quad (13)$$

$$R = \begin{bmatrix} 1 & 0.9891 & 0.9566 & 0.9037 \\ 0.9891 & 1 & 0.9891 & 0.9566 \\ 0.9566 & 0.9326 & 1 & 0.989 \\ 0.9037 & 0.9566 & 0.9891 & 1 \end{bmatrix} \quad (14)$$

$$R = \begin{bmatrix} 1 & 0.9973 & 0.9891 & 0.9755 \\ 0.9973 & 1 & 0.9973 & 0.9891 \\ 0.9891 & 0.9973 & 1 & 0.9973 \\ 0.9755 & 0.9891 & 0.9973 & 1 \end{bmatrix} \quad (15)$$

The normalized correlation matrix R is used to obtain the simulation results as shown below.

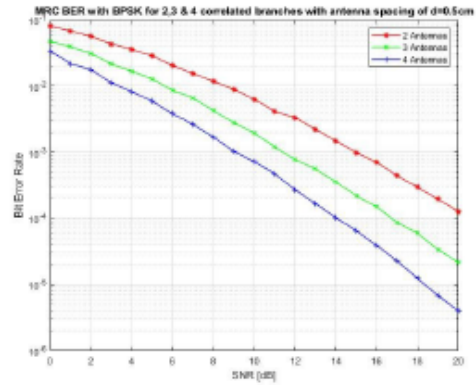


Figure 1 - MRC BER with BPSK for 2,3 & 4 correlated branches with antenna spacing of  $d=0.5\text{cm}$

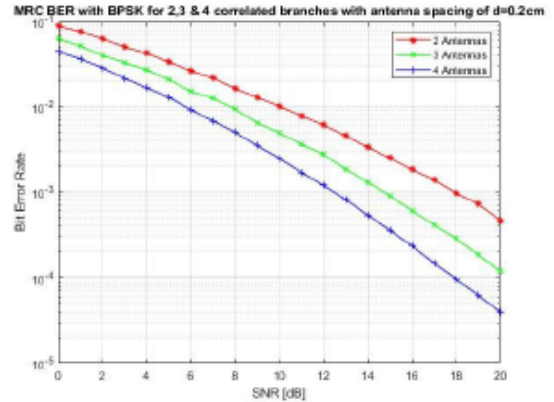


Figure 2 - MRC BER with BPSK for 2,3 & 4 correlated branches with antenna spacing of  $d=0.2\text{cm}$

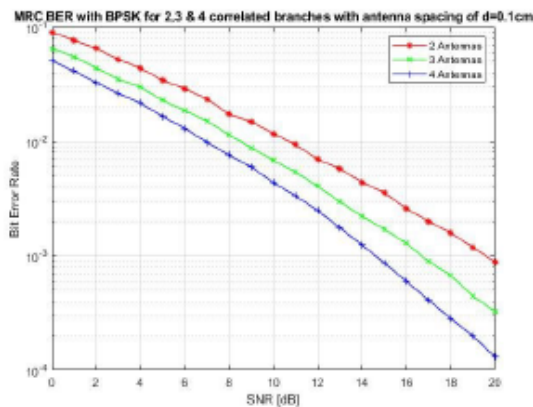


Figure 3 - MRC BER with BPSK for 2,3 & 4 correlated branches with antenna spacing of  $d=0.1\text{cm}$

## V. CONCLUSION

From the simulation results, it can be seen that the higher the number of antennas at the receiver the better the reception diversity. This has been done for different antenna spacing and it can be seen that if they are too close together then the BER is slightly higher as compared to when they are slightly apart. Using this, various simulations are be done to find the maximum permissible separation distance for the antennas that will allow for faster data rates which in this case is 0.5cm.

5G having several frequencies ranges, further work can be done by simulating the same for various frequencies and comparing the BER vs SNR plots to find the most optimal separation distance that achieves faster data rates at the selected frequencies.

## REFERENCES

- [1] M. K. Simon and M. S. Alouini, *Digital Communication over Fading Channels*, John Wiley & Sons, New York, NY, USA, 2005.
- [2] D. Skraparis, V. K. Sakarellos, A. D. Panagopoulos, and J. D. Kanellopoulos, "Performance of N-branch receive diversity combining in correlated lognormal channels," *IEEE Communications Letters*, vol. 13, no. 7, pp. 489–491, 2009.
- [3] G. K. Karagiannidis, D. A. Zogas, N. C. Sagias, S. A. Kotsopoulos, and G. S. Tombras, "Equal-gain and maximal-ratio combining over nonidentical weibull fading channels," *IEEE Transactions on Wireless Communications*, vol. 4, no. 3, pp. 841–846, 2005.
- [4] R. Annavajjala and L. B. Milstein, "Performance analysis of linear diversity-combining schemes on Rayleigh fading channels with binary signaling and Gaussian weighting errors," *IEEE Transactions on Wireless Communications*, vol. 4, no. 5, pp. 2267–2277, 2005.
- [5] Brennan, D.G.: 'Linear diversity combining techniques. Proc. IRE, 1959, vol. 47, pp. 1075–1102

- [6] M. K. Simon and M.-S. Alouini, *Digital Communication over Fading Channels*, vol. 95, John Wiley & Sons, New York, NY, USA, 2005.
- [7] E. A. Lee and D. G. Messerschmitt, *Digital Communications*, Springer, New York, NY, USA, 2004.
- [8] R. K. Mallik and J. H. Winters, "Deterministic linear combining receivers for random fading channels," *IEEE Transactions on Communications*, vol. 58, no. 9, pp. 2630–2638, 2010.
- [9] F. S. Al-Qahtani, S. A. Zummo, A. K. Gurung, and Z. M. Hussain, "Spectral efficiency of maximum ratio combining (MRC) over slow fading with estimation errors," *Digital Signal Processing*, vol. 20, no. 1, pp. 85–96, 2010.
- [10] K. S. Ahn and R. W. Heath Jr., "Performance analysis of maximum ratio combining with imperfect channel estimation in the presence of cochannel interferences," *IEEE Transactions on Wireless Communications*, vol. 8, no. 3, pp. 1080–1085, 2009.
- [11] S. Roy and P. Fortier, "Maximal-ratio combining architectures and performance with channel estimation based on a training sequence," *IEEE Transactions on Wireless Communications*, vol. 3, no. 4, pp. 1154–1164, 2004.
- [12] S. Verdú, *Multuser Detection*, Cambridge University Press, New York, NY, USA, 1998.
- [13] L. C. Godara, Ed., *Handbook of Antennas in Wireless Communications*, CRC Press, Boca Raton, Fla, USA, 2001.
- [14] Horn, R.A., Johnson, C.R.: 'Matrix analysis' (Cambridge University Press, Cambridge, UK, 1990)
- [15] R. You, H. Li, and Y. Bar-Ness, "Diversity combining with imperfect channel estimation," *IEEE Transactions on Communications*, vol. 53, no. 10, pp. 1655–1662, 2005.
- [16] N. Kong, T. Eng, and L. B. Milstein, "A selection combining scheme for RAKE receivers," in *Proceedings of the IEEE International Conference on Universal Personal Communications (ICUPC '95)*, pp. 426–429, Tokyo, Japan, November 1995.
- [17] T. Eng, N. Kong, and L. B. Milstein, "Comparison of diversity combining techniques for Rayleigh-fading channels," *IEEE Transactions on Communications*, vol. 44, no. 9, pp. 1117–1129, 1996.
- [18] M. Z. Win and J. H. Winters, "Analysis of hybrid selection/maximal-ratio combining in Rayleigh fading," *IEEE Transactions on Communications*, vol. 47, no. 12, pp. 1773–1776, 1999.
- [19] Dinamani, S. Das, L. Bijendra, R. Shruti, S. Babina, and B. Kiran, "Performance of a hybrid MRC/SC diversity receiver over Rayleigh fading channel," in *Proceedings of the International Conference on Circuits, Controls and Communications (CCUBE '13)*, pp. 1–4, IEEE, 2013.
- [20] J. Cui and A. U. H. Sheikh, "Outage probability of cellular radio systems using maximal ratio combining in the presence of multiple interferers," *IEEE Transactions on Communications*, vol. 47, no. 8, pp. 1121–1124, 1999.
- [21] V. A. Aalo and J. Zhang, "On the effect of cochannel interference on average error rates in Nakagami-fading channels," *IEEE Communications Letters*, vol. 3, no. 5, pp. 136–138, 1999.
- [22] Shah and A. M. Haimovich, "Performance analysis of maximal ratio combining and comparison with optimum combining for mobile radio communications with cochannel interference," *IEEE Transactions on Vehicular Technology*, vol. 49, no. 4, pp. 1454–1463, 2000.
- [23] J. P. Pena-Martin, J. M. Romero-Jerez, G. Aguilera, and A. J. Goldsmith, "Performance comparison of MRC and IC under transmit diversity," *IEEE Transactions on Wireless Communications*, vol. 8, no. 5, pp. 2484–2493, 2009.
- [24] X. Zhang and N. C. Beaulieu, "Explicit analytical expressions for outage and error rate of diversity cellular systems in the presence of multiple interferers and correlated Rayleigh fading," *IEEE Transactions on Communications*, vol. 55, no. 12, pp. 2303–2315, 2007.
- [25] R. M. Radsydeh, "MRC in the presence of asynchronous cochannel interference over frequency-selective Rayleigh fading channels," *IEEE Transactions on Vehicular Technology*, vol. 58, no. 8, pp. 4329–4341, 2009.

- [26] M. J. Gans, "The effect of Gaussian error in maximal ratio combiners," *IEEE Transactions on Communications*, vol. 19, no. 4, pp. 492–500, 1971.
- [27] R. Annavajjala and L. B. Milstein, "Performance analysis of linear diversity-combining schemes on Rayleigh fading channels with binary signaling and Gaussian weighting errors," *IEEE Transactions on Wireless Communications*, vol. 4, no. 5, pp. 2267–2277, 2005.
- [28] Y. Ma, R. Schober, and D. Zhang, "Exact BER for M-QAM with MRC and imperfect channel estimation in Rician fading channels," *IEEE Transactions on Wireless Communications*, vol. 6, no. 3, pp. 926–936, 2007.
- [29] L. Najafizadeh and C. Tellambura, "BER analysis of arbitrary QAM for MRC diversity with imperfect channel estimation in generalized Ricean fading channels," *IEEE Transactions on Vehicular Technology*, vol. 55, no. 4, pp. 1239–1248, 2006.
- [30] R. Annavajjala, P. C. Cosman, and L. B. Milstein, "Performance analysis of linear modulation schemes with generalized diversity combining on Rayleigh fading channels with noisy channel estimates," *IEEE Transactions on Information Theory*, vol. 53, no. 12, pp. 4701–4727, 2007.
- [31] W. M. Gifford, M. Z. Win, and M. Chiani, "Antenna subset diversity with non-ideal channel estimation," *IEEE Transactions on Wireless Communications*, vol. 7, no. 5, pp. 1527–1539, 2008.
- [32] S. Roy and P. Fortier, "Maximal-ratio combining architectures and performance with channel estimation based on a training sequence," *IEEE Transactions on Wireless Communications*, vol. 3, no. 4, pp. 1154–1164, 2004.
- [33] Y. Tokgoz and B. D. Rao, "The effect of imperfect channel estimation on the performance of maximum ratio combining in the presence of cochannel interference," *IEEE Transactions on Vehicular Technology*, vol. 55, no. 5, pp. 1527–1534, 2006.
- [34] K. S. Ahn and R. W. Heath Jr., "Performance analysis of maximum ratio combining with imperfect channel estimation in the presence of cochannel interferences," *IEEE Transactions on Wireless Communications*, vol. 8, no. 3, pp. 1080–1085, 2009.
- [35] R. Annavajjala and L. B. Milstein, "Performance analysis of linear diversity-combining schemes on Rayleigh fading channels with binary signaling and Gaussian weighting errors," *IEEE Transactions on Wireless Communications*, vol. 4, no. 5, pp. 2267–2277, 2005.
- [36] M. Akbari, M. R. Hossain, M. R. Manesh, A. A. El-Saleh, and A. M. Kareem, "Minimizing sensing decision error in cognitive radio networks using evolutionary algorithms," *KSII Transactions on Internet and Information Systems*, vol. 6, no. 9, pp. 2037–2051, 2012.